Supporting Information

A dynamic switch in inactive p38γ leads to an excited state on pathway to an active kinase

Phillip C. Aoto[†,‡], Robyn L. Stanfield[†], Ian A. Wilson[†,§], H. Jane Dyson[†], Peter E. Wright[†,§,]*

[†]Department of Integrative Structural and Computational Biology, and [§] The Skaggs Institute for Chemical Biology, The Scripps Research Institute, 10550 North Torrey Pines Road, La Jolla CA 92037.

[§]Present address: Department of Pharmacology, University of California, San Diego, 9500 Gilman Dr, La Jolla, CA 92093

Table S1. Data collection and refinement statistics

	inactive p38γ
Data collection	
Beamline	APS-23-ID-D
Wavelength (Å)	1.03316
Resolution range (Å)	44.59-2.55 (2.62-2.55)
Space group	P1
Unit cell dimensions (Å, °)	47.03, 66.36, 68.57, 115.27, 102.49, 96.83
Total reflections	43042(2007)
Unique reflections	22388(1051)
Rmerge(I)[b]	0.075(0.37)
Rmeas[c]	0.11(0.53)
Rpim[d]	0.075(0.37)
CC1/2[e]	0.91(0.68)
Completeness (%)	98.1(92.9)
Multiplicity	1.9(1.9)
<I>/<σ(I)>	10.3 (2.2)
Refinement	
Reflections used for Rwork(Rfree)	21274(1112)
Number of protein atoms	5377
Number of waters	45
Number of sulfates	2
Rwork	0.19(0.27)
Rfree	0.25(0.34)
Average B-value (Å^2)	50
Wilson B-value (Å^2)	42
RMSD from ideality	
Bond length (Å)	0.003
Bond angle (°)	0.584
Clashscore	3.6
Ramachandran plot	
Favored (%)	96
Allowed (%)	4
Outlier (%)	0

[a]Numbers in parentheses are for highest resolution shell

[b]$R_{merge} = \Sigma_{hkl}\Sigma_{i=1,n}|I_i(hkl) - \langle I(hkl)\rangle| / \Sigma_{hkl}\Sigma_{i=1,n}I_i(hkl)$

[c]$R_{meas} = \Sigma_{hkl}\sqrt{(n/n-1)}\ \Sigma_{i=1,n}|I_i(hkl) - \langle I(hkl)\rangle| / \Sigma_{hkl}\Sigma_{i=1,n}I_i(hkl)$

[d]$R_{pim} = \Sigma_{hkl}\sqrt{(1/n-1)}\ \Sigma_{i=1,n}|I_i(hkl) - \langle I(hkl)\rangle| / \Sigma_{hkl}\Sigma_{i=1,n}I_i(hkl)$

[e]$CC_{1/2}$ = Pearson Correlation Coefficient between two random half datasets

[f]Number of unfavorable all-atom steric overlaps ≥ 0.4Å per 1000 atoms

Table S2. ^{15}N Relaxation data.

Backbone Amide	R_1(1/s) 500MHz	R_1(1/s) 800MHz	R_2(1/s) 500MHz	R_2(1/s) 800MHz	{^{1}H}-^{15}N NOE 500MHz	{^{1}H}-^{15}N NOE 800MHz
7	1.01 (0.01)	0.90 (0.01)	17.16 (0.06)	21.82 (0.1)	0.30 (0.02)	0.35 (0.03)
8	0.83 (0.03)	0.60 (0.02)	31.52 (0.21)	39.14 (0.33)	0.41 (0)	0.49 (0.1)
9	0.73 (0.03)	0.46 (0.02)	30.68 (0.21)	37.92 (0.36)	0.53 (0.02)	0.63 (0.04)
10	0.67 (0.09)	0.29 (0.17)	38.02 (0.47)	49.17 (1.78)	0.64 (0.26)	-0.44 (0.81)
11	0.57 (0.03)	0.37 (0.02)	40.31 (0.3)	57.87 (0.58)	0.64 (0.17)	0.76 (0.09)
12	0.43 (0.03)	0.30 (0.02)	49.75 (0.34)	58.20 (0.6)	0.63 (0.11)	0.81 (0.08)
13	0.53 (0.02)	0.31 (0.01)	42.13 (0.18)	61.27 (0.37)	0.85 (0.12)	0.85 (0.12)
14	0.54 (0.03)	0.37 (0.02)	36.64 (0.19)	44.29 (0.42)	0.78 (0.01)	0.70 (0.06)
15	0.60 (0.02)	0.33 (0.01)	36.83 (0.15)	52.33 (0.33)	0.66 (0.08)	0.61 (0.03)
16	0.61 (0.03)	0.36 (0.02)	33.30 (0.21)	40.22 (0.52)	0.68 (0.08)	0.70 (0.01)
18	0.59 (0.06)	0.43 (0.05)	36.89 (0.47)	54.32 (1.24)	0.46 (0.08)	0.63 (0.08)
19	0.70 (0.03)	0.45 (0.02)	29.27 (0.18)	39.41 (0.39)	0.59 (0.02)	0.51 (0.07)
20	0.62 (0.03)	0.37 (0.02)	32.98 (0.23)	44.69 (0.56)	0.50 (0.06)	0.52 (0.15)
21	0.59 (0.03)	0.34 (0.01)	35.91 (0.18)	47.42 (0.34)	0.61 (0.04)	0.71 (0)
22	0.58 (0.05)	0.24 (0.03)	40.22 (0.38)	52.17 (0.85)	0.68 (0.07)	0.71 (0.13)
23	0.54 (0.03)	0.26 (0.02)	36.96 (0.25)	46.02 (0.41)	0.78 (0.17)	0.70 (0.03)
25	0.55 (0.02)	0.37 (0.01)	30.95 (0.18)	47.74 (0.38)	0.64 (0.1)	0.83 (0.06)
26	0.55 (0.03)	0.29 (0.02)	34.05 (0.28)	52.16 (0.57)	0.77 (0.05)	0.74 (0.08)
27	0.52 (0.02)	0.30 (0.01)	38.00 (0.15)	57.84 (0.31)	0.78 (0.06)	0.84 (0.04)
28	0.53 (0.03)	0.29 (0.02)	38.23 (0.26)	48.56 (0.47)	0.73 (0.05)	0.69 (0.06)
29	0.47 (0.02)	0.28 (0.01)	46.07 (0.19)	56.19 (0.34)	0.55 (0.02)	0.70 (0.02)
30	0.51 (0.02)	0.27 (0.01)	41.47 (0.21)	62.08 (0.48)	0.69 (0.01)	0.77 (0.01)
31	0.65 (0.02)	0.32 (0.01)	25.41 (0.21)	42.78 (0.41)	0.66 (0.11)	0.81 (0)
36	0.60 (0.03)	0.39 (0.02)	29.41 (0.21)	41.03 (0.47)	0.39 (0)	0.47 (0.04)
38	0.52 (0.07)	0.49 (0.06)	29.66 (0.6)	59.51 (1.47)	0.79 (0.28)	0.90 (0.07)
42	0.61 (0.04)	0.32 (0.03)	33.51 (0.28)	57.82 (0.76)	0.73 (0.03)	0.86 (0.18)
43	0.56 (0.04)	0.34 (0.02)	36.52 (0.3)	48.05 (0.56)	0.73 (0.01)	0.66 (0.07)
45	0.49 (0.03)	0.27 (0.02)	38.96 (0.28)	52.23 (0.52)	0.64 (0.17)	1.01 (0.05)
46	0.52 (0.02)	0.27 (0.01)	40.95 (0.2)	56.39 (0.41)	0.74 (0.03)	0.74 (0.01)
47	0.57 (0.03)	0.30 (0.02)	36.24 (0.23)	50.25 (0.47)	0.78 (0.02)	0.71 (0)
48	0.54 (0.04)	0.33 (0.03)	37.43 (0.33)	54.21 (0.64)	0.77 (0.09)	0.67 (0.06)
50	0.53 (0.08)	0.31 (0.04)	29.16 (0.68)	48.08 (1.22)	0.59 (0.09)	0.55 (0.16)
51	0.50 (0.03)	0.36 (0.02)	36.37 (0.26)	56.09 (0.53)	0.65 (0.07)	0.72 (0.09)
52	0.63 (0.01)	0.34 (0.01)	30.61 (0.09)	38.22 (0.23)	0.42 (0)	0.50 (0.05)
57	0.58 (0.04)	0.26 (0.03)	38.49 (0.29)	51.29 (0.69)	0.88 (0.03)	0.77 (0.05)
58	0.57 (0.05)	0.33 (0.04)	38.82 (0.38)	45.70 (0.93)	0.91 (0.13)	0.73 (0.01)
59	0.50 (0.03)	0.35 (0.02)	33.10 (0.24)	48.56 (0.51)	0.73 (0.1)	0.71 (0.18)
60	0.57 (0.05)	0.24 (0.06)	36.76 (0.34)	57.12 (1.42)	0.54 (0.15)	0.89 (0.11)
62	0.50 (0.03)	0.37 (0.02)	31.81 (0.31)	48.58 (0.58)	0.50 (0.16)	0.94 (0.12)
63	0.41 (0.04)	0.38 (0.03)	42.55 (0.38)	62.13 (1.98)	0.78 (0.06)	0.77 (0.07)
68	0.63 (0.05)	0.33 (0.02)	39.53 (0.32)	45.62 (0.61)	0.65 (0.13)	0.69 (0.17)
69	0.55 (0.04)	0.29 (0.03)	38.59 (0.32)	61.36 (0.76)	0.73 (0.06)	0.79 (0.03)
70	0.54 (0.08)	0.36 (0.08)	34.49 (0.55)	50.19 (2.11)	0.65 (0.09)	0.74 (0.17)
83	0.66 (0.01)	0.46 (0.01)	29.79 (0.06)	37.94 (0.28)	0.45 (0.01)	0.67 (0.05)
84	0.56 (0.02)	0.30 (0.02)	34.84 (0.22)	49.36 (0.4)	0.98 (0.01)	0.75 (0.12)
85	0.51 (0.05)	0.32 (0.04)	34.52 (0.47)	41.64 (0.95)	0.70 (0.11)	0.89 (0.04)

Table S2 continued. ^{15}N Relaxation data.

Backbone Amide	R_1(1/s) 500MHz	R_1(1/s) 800MHz	R_2(1/s) 500MHz	R_2(1/s) 800MHz	{^1H}-^{15}N NOE 500MHz	{^1H}-^{15}N NOE 800MHz
86	0.59 (0.03)	0.30 (0.02)	31.23 (0.23)	55.60 (0.61)	0.65 (0.01)	0.83 (0.04)
87	0.56 (0.05)	0.34 (0.05)	36.02 (0.41)	59.13 (1.12)	0.93 (0.08)	0.70 (0.04)
88	0.60 (0.04)	0.37 (0.04)	31.06 (0.32)	52.37 (1)	0.48 (0.13)	0.77 (0.02)
89	0.55 (0.02)	0.36 (0.02)	32.04 (0.21)	46.74 (0.47)	0.58 (0.03)	0.76 (0.08)
90	0.68 (0.09)	0.37 (0.06)	34.87 (0.56)	44.77 (1.07)	1.00 (0.38)	0.84 (0.28)
94	0.56 (0.02)	0.29 (0.01)	41.84 (0.19)	47.36 (0.35)	0.72 (0.12)	0.90 (0.01)
96	0.50 (0.04)	0.27 (0.03)	19.59 (0.23)	40.60 (0.61)	0.61 (0.05)	0.73 (0.07)
97	0.61 (0.03)	0.38 (0.02)	35.73 (0.24)	47.66 (0.4)	0.55 (0.09)	0.56 (0.1)
98	0.58 (0.03)	0.39 (0.02)	33.39 (0.25)	50.02 (0.5)	0.59 (0.11)	0.52 (0.01)
100	0.52 (0.03)	0.35 (0.02)	41.96 (0.33)	61.36 (0.5)	0.74 (0.05)	0.73 (0.06)
101	0.61 (0.06)	0.30 (0.03)	37.19 (0.5)	45.00 (0.75)	0.58 (0.04)	0.46 (0.11)
102	0.47 (0.03)	0.33 (0.02)	31.37 (0.28)	49.90 (0.53)	0.88 (0.19)	0.52 (0.14)
103	0.53 (0.1)	0.25 (0.06)	30.45 (0.84)	53.65 (1.71)	0.89 (0.43)	0.65 (0.07)
111	0.54 (0.03)	0.36 (0.02)	31.77 (0.24)	64.22 (0.71)	0.69 (0.09)	0.63 (0.13)
112	0.96 (0.06)	0.53 (0.1)	27.90 (0.32)	40.93 (1.44)	0.65 (0.29)	0.53 (0.26)
114	0.58 (0.02)	0.39 (0.02)	35.04 (0.17)	44.49 (0.38)	0.71 (0.09)	0.75 (0.09)
115	0.58 (0.03)	0.41 (0.02)	34.15 (0.26)	46.76 (0.62)	0.56 (0.06)	0.77 (0.15)
116	0.54 (0.03)	0.29 (0.02)	38.85 (0.3)	50.71 (0.56)	0.82 (0.14)	0.85 (0.04)
118	0.51 (0.05)	0.24 (0.03)	37.51 (0.43)	51.29 (0.75)	0.70 (0.11)	0.80 (0)
120	0.60 (0.03)	0.41 (0.02)	34.55 (0.31)	42.44 (0.57)	0.60 (0.07)	0.72 (0.03)
121	0.58 (0.03)	0.32 (0.02)	39.40 (0.31)	48.50 (0.45)	0.47 (0.05)	0.62 (0.09)
122	0.70 (0.04)	0.44 (0.03)	29.59 (0.33)	45.25 (0.6)	0.36 (0.17)	0.41 (0.02)
123	0.72 (0.02)	0.55 (0.01)	27.22 (0.13)	39.51 (0.22)	0.43 (0.06)	0.52 (0.01)
125	0.70 (0.01)	0.54 (0.01)	28.03 (0.11)	41.56 (0.21)	0.19 (0.06)	0.32 (0.06)
126	0.58 (0.02)	0.40 (0.01)	39.73 (0.16)	47.85 (0.3)	0.66 (0.05)	0.75 (0.03)
127	0.60 (0.04)	0.40 (0.02)	38.05 (0.34)	52.47 (0.6)	0.92 (0.13)	0.68 (0.03)
130	0.59 (0.04)	0.37 (0.02)	26.54 (0.29)	49.40 (0.51)	0.72 (0.02)	0.85 (0.16)
131	0.56 (0.03)	0.28 (0.02)	34.22 (0.21)	47.18 (0.47)	0.75 (0.03)	0.90 (0.09)
132	0.50 (0.02)	0.32 (0.01)	38.62 (0.21)	55.68 (0.4)	0.77 (0.05)	0.70 (0.05)
133	0.65 (0.04)	0.55 (0.03)	26.73 (0.26)	38.80 (0.68)	0.43 (0.05)	0.61 (0.04)
135	0.79 (0.11)	0.38 (0.08)	39.78 (1)	48.41 (2.56)	0.69 (0.35)	0.82 (0.21)
147	0.50 (0.1)	0.31 (0.05)	33.97 (0.57)	40.30 (1.09)	0.55 (0.12)	0.88 (0.22)
148	0.51 (0.03)	0.28 (0.02)	45.42 (0.34)	48.73 (0.73)	0.83 (0.16)	0.77 (0.03)
158	0.55 (0.02)	0.40 (0.02)	36.32 (0.19)	43.54 (0.48)	0.82 (0.21)	0.71 (0.09)
159	0.43 (0.07)	0.20 (0.05)	29.15 (0.49)	51.61 (1.1)	0.56 (0.02)	0.84 (0.01)
161	0.44 (0.03)	0.36 (0.04)	38.99 (0.37)	49.87 (0.83)	0.77 (0.12)	0.72 (0.09)
162	0.52 (0.02)	0.30 (0.01)	30.27 (0.14)	55.00 (0.31)	0.74 (0.02)	0.85 (0.01)
163	0.59 (0.04)	0.34 (0.03)	44.71 (0.39)	48.73 (0.7)	0.42 (0.01)	0.54 (0.06)
164	0.51 (0.04)	0.35 (0.02)	31.15 (0.37)	46.84 (0.59)	0.58 (0)	0.54 (0.06)
165	0.64 (0.06)	0.27 (0.03)	47.81 (0.59)	52.35 (0.8)	0.61 (0.1)	0.68 (0.07)
166	0.51 (0.02)	0.30 (0.02)	45.85 (0.25)	51.07 (0.55)	0.72 (0)	0.79 (0.01)
167	0.54 (0.04)	0.27 (0.03)	39.37 (0.35)	47.67 (0.6)	0.79 (0.12)	0.70 (0.07)
168	0.50 (0.08)	0.50 (0.1)	48.36 (0.6)	42.10 (1.66)	0.77 (0.03)	0.64 (0.09)
172	0.61 (0.03)	0.48 (0.03)	31.64 (0.21)	42.10 (0.48)	0.62 (0)	0.46 (0.02)
173	0.51 (0.15)	0.27 (0.1)	31.61 (1.83)	58.95 (4.22)	0.83 (0.2)	0.51 (0.17)

Table S2 continued. ^{15}N Relaxation data.

Backbone Amide	R_1(1/s) 500MHz	R_1(1/s) 800MHz	R_2(1/s) 500MHz	R_2(1/s) 800MHz	{^{1}H}-^{15}N NOE 500MHz	{^{1}H}-^{15}N NOE 800MHz
175	0.70 (0.01)	0.47 (0.01)	31.39 (0.09)	41.89 (0.17)	0.56 (0.04)	0.70 (0.01)
176	0.68 (0.01)	0.48 (0.01)	30.51 (0.08)	43.80 (0.15)	0.34 (0.02)	0.34 (0.05)
179	0.75 (0.04)	0.42 (0.08)	30.88 (0.23)	46.86 (1.65)	0.64 (0.13)	0.62 (0.11)
181	0.74 (0.04)	0.53 (0.03)	19.49 (0.26)	34.24 (0.54)	0.64 (0)	0.72 (0.07)
182	0.74 (0.07)	0.48 (0.13)	22.47 (0.38)	35.46 (1.81)	0.47 (0.05)	0.76 (0.15)
185	0.76 (0.02)	0.42 (0.01)	26.46 (0.15)	35.11 (0.31)	0.67 (0.11)	0.79 (0.02)
186	1.02 (0.04)	0.76 (0.04)	26.44 (0.2)	42.08 (0.61)	0.45 (0.1)	0.68 (0.08)
206	0.42 (0.07)	0.27 (0.06)	27.84 (0.74)	48.15 (1.73)	0.95 (0.11)	0.70 (0.14)
209	0.54 (0.05)	0.32 (0.05)	36.77 (0.34)	56.36 (1.35)	0.77 (0.02)	0.69 (0.06)
212	0.72 (0.06)	0.42 (0.11)	30.27 (0.33)	38.19 (1.58)	0.76 (0.1)	0.60 (0.06)
217	0.53 (0.03)	0.33 (0.02)	37.53 (0.25)	51.83 (0.48)	0.82 (0.02)	0.82 (0.07)
220	0.51 (0.02)	0.32 (0.02)	45.85 (0.25)	55.61 (0.4)	0.73 (0.02)	0.70 (0.05)
221	0.61 (0.06)	0.20 (0.03)	25.86 (0.57)	42.68 (1.15)	0.80 (0.08)	0.69 (0.08)
222	0.65 (0.03)	0.39 (0.02)	32.65 (0.25)	44.94 (0.47)	0.73 (0.12)	0.66 (0.03)
223	0.60 (0.03)	0.31 (0.02)	28.91 (0.24)	44.45 (0.55)	0.73 (0.04)	0.73 (0.03)
224	0.58 (0.02)	0.38 (0.01)	32.00 (0.16)	42.65 (0.34)	0.74 (0.07)	0.57 (0.16)
233	0.48 (0.05)	0.28 (0.05)	38.87 (0.43)	56.62 (1.2)	0.76 (0.17)	0.73 (0.23)
234	0.55 (0.06)	0.47 (0.06)	38.23 (0.5)	46.25 (1.52)	0.72 (0.06)	0.87 (0.11)
241	0.59 (0.03)	0.33 (0.02)	43.17 (0.26)	54.73 (0.57)	0.67 (0.19)	0.69 (0.02)
243	0.54 (0.06)	0.35 (0.05)	39.56 (0.62)	46.18 (1.37)	0.63 (0.01)	0.66 (0.3)
247	0.53 (0.03)	0.31 (0.02)	42.47 (0.32)	64.39 (0.77)	0.61 (0.06)	0.53 (0.08)
248	0.72 (0.06)	0.32 (0.06)	36.53 (0.44)	43.81 (1.6)	0.35 (0.07)	0.88 (0.2)
249	0.61 (0.08)	0.26 (0.09)	30.03 (0.66)	48.87 (2.36)	0.44 (0.17)	0.82 (0.2)
251	0.49 (0.03)	0.42 (0.04)	38.15 (0.32)	51.97 (0.83)	0.67 (0)	0.67 (0.04)
252	0.53 (0.03)	0.35 (0.03)	38.37 (0.27)	36.34 (0.6)	0.52 (0.04)	0.80 (0.02)
253	0.54 (0.05)	0.28 (0.05)	33.93 (0.34)	56.36 (1.35)	0.77 (0.02)	0.98 (0.21)
259	0.64 (0.04)	0.31 (0.03)	33.51 (0.34)	47.28 (0.8)	0.73 (0.1)	0.75 (0.04)
260	0.59 (0.02)	0.37 (0.01)	38.58 (0.17)	49.21 (0.36)	0.70 (0.03)	0.81 (0.05)
261	0.60 (0.03)	0.38 (0.02)	31.11 (0.23)	55.28 (0.59)	0.66 (0.02)	0.61 (0.04)
262	0.79 (0.06)	0.54 (0.06)	38.75 (0.44)	49.53 (1.41)	0.69 (0.01)	0.75 (0.02)
263	0.56 (0.04)	0.38 (0.03)	37.25 (0.28)	50.91 (0.74)	0.53 (0.06)	0.68 (0.02)
264	0.57 (0.06)	0.24 (0.08)	35.41 (0.63)	47.06 (1.87)	0.46 (0.08)	0.69 (0.04)
265	0.64 (0.02)	0.41 (0.02)	31.52 (0.17)	43.29 (0.41)	0.51 (0.01)	0.49 (0.08)
267	0.68 (0.01)	0.48 (0.01)	30.51 (0.08)	43.80 (0.15)	0.35 (0.01)	0.34 (0.05)
268	0.76 (0.06)	0.51 (0.08)	28.01 (0.35)	39.22 (1.24)	0.51 (0.08)	0.91 (0.32)
269	0.74 (0.02)	0.54 (0.01)	29.93 (0.11)	36.97 (0.24)	0.39 (0.03)	0.47 (0.04)
270	0.66 (0.01)	0.49 (0.01)	26.78 (0.06)	40.98 (0.13)	0.42 (0.04)	0.54 (0)
271	0.65 (0.02)	0.39 (0.02)	33.73 (0.16)	44.44 (0.35)	0.48 (0.05)	0.63 (0.05)
273	0.68 (0.04)	0.34 (0.03)	38.94 (0.34)	55.50 (1.04)	0.46 (0.08)	0.56 (0.19)
274	0.60 (0.03)	0.42 (0.02)	41.31 (0.24)	51.52 (0.44)	0.88 (0.05)	0.69 (0.13)
275	0.59 (0.04)	0.36 (0.02)	31.63 (0.32)	43.91 (0.54)	0.44 (0.09)	0.67 (0.07)
277	0.50 (0.03)	0.35 (0.02)	33.09 (0.24)	48.56 (0.51)	0.73 (0.1)	0.71 (0.18)
279	0.59 (0.04)	0.47 (0.02)	32.81 (0.27)	44.58 (0.48)	0.36 (0.09)	0.30 (0.04)
280	0.60 (0.02)	0.41 (0.01)	31.03 (0.13)	42.52 (0.24)	0.46 (0.03)	0.34 (0.02)
281	0.53 (0.02)	0.34 (0.01)	37.95 (0.18)	50.98 (0.36)	0.44 (0.06)	0.51 (0.12)

Table S2 continued. ^{15}N Relaxation data.

Backbone Amide	R_1(1/s) 500MHz	R_1(1/s) 800MHz	R_2(1/s) 500MHz	R_2(1/s) 800MHz	{^{1}H}-^{15}N NOE 500MHz	{^{1}H}-^{15}N NOE 800MHz
283	0.62 (0.03)	0.47 (0.02)	30.41 (0.22)	42.47 (0.46)	0.59 (0.03)	0.67 (0)
284	0.49 (0.05)	0.28 (0.02)	35.77 (0.41)	48.98 (0.71)	0.86 (0.03)	0.87 (0)
285	0.47 (0.04)	0.30 (0.02)	32.19 (0.36)	48.58 (0.65)	0.98 (0.05)	0.90 (0.13)
286	0.54 (0.02)	0.37 (0.01)	40.28 (0.18)	50.27 (0.32)	0.90 (0.06)	0.72 (0.01)
287	0.57 (0.06)	0.37 (0.05)	36.85 (0.51)	41.44 (1.14)	0.73 (0.08)	0.82 (0.09)
288	0.68 (0.12)	0.55 (0.07)	23.08 (0.71)	44.22 (2.06)	0.77 (0.17)	0.70 (0.01)
294	0.54 (0.04)	0.36 (0.05)	44.71 (0.41)	66.74 (1.41)	0.64 (0.15)	0.89 (0.16)
295	0.51 (0.02)	0.33 (0.03)	37.66 (0.24)	51.46 (0.82)	0.67 (0.09)	0.73 (0.06)
298	0.54 (0.02)	0.37 (0.01)	40.28 (0.18)	50.27 (0.32)	0.90 (0.06)	0.72 (0.01)
299	0.62 (0.04)	0.36 (0.03)	31.48 (0.29)	50.93 (0.71)	0.85 (0.21)	0.62 (0.11)
300	0.53 (0.03)	0.31 (0.02)	41.04 (0.26)	44.10 (0.42)	0.46 (0.06)	0.75 (0.01)
301	0.44 (0.04)	0.24 (0.02)	41.85 (0.4)	56.63 (0.73)	0.65 (0.03)	0.96 (0.39)
303	0.52 (0.04)	0.27 (0.04)	33.55 (0.31)	44.92 (0.71)	0.69 (0.06)	0.70 (0.06)
304	0.54 (0.04)	0.29 (0.02)	37.76 (0.35)	59.04 (0.69)	0.57 (0.08)	0.67 (0.05)
306	0.48 (0.03)	0.37 (0.02)	37.70 (0.28)	57.88 (0.92)	0.96 (0.11)	0.78 (0.11)
307	0.70 (0.08)	0.44 (0.05)	34.38 (0.51)	41.62 (1)	0.50 (0.09)	0.56 (0.12)
310	0.60 (0.03)	0.29 (0.02)	37.40 (0.23)	50.04 (0.56)	0.93 (0.1)	0.75 (0.13)
312	0.49 (0.02)	0.32 (0.01)	39.38 (0.21)	60.52 (0.38)	0.67 (0.04)	0.64 (0.12)
313	0.65 (0.03)	0.39 (0.02)	32.65 (0.25)	44.94 (0.47)	0.73 (0.12)	0.66 (0.03)
315	0.51 (0.02)	0.32 (0.01)	45.85 (0.25)	55.68 (0.4)	0.77 (0.05)	0.74 (0)
316	1.09 (0.01)	0.85 (0.01)	17.59 (0.06)	24.16 (0.12)	0.24 (0.07)	0.40 (0)
318	1.09 (0.01)	0.85 (0.01)	17.59 (0.06)	23.48 (0.13)	0.23 (0.08)	0.46 (0.01)
319	1.09 (0.01)	0.85 (0.01)	17.59 (0.06)	24.16 (0.12)	0.24 (0.07)	0.40 (0)
320	1.04 (0.01)	0.85 (0.01)	16.78 (0.04)	21.07 (0.07)	0.18 (0.03)	0.32 (0)
322	1.02 (0.03)	0.68 (0.01)	20.63 (0.14)	24.72 (0.23)	0.25 (0.03)	0.44 (0.02)
323	0.73 (0.02)	0.56 (0.01)	25.61 (0.1)	34.95 (0.2)	0.16 (0.01)	0.14 (0.04)
324	0.74 (0.02)	0.51 (0.01)	33.04 (0.1)	38.59 (0.2)	0.48 (0.05)	0.40 (0.04)
325	0.63 (0.01)	0.36 (0.01)	30.59 (0.11)	42.90 (0.19)	0.64 (0.09)	0.52 (0.06)
326	0.54 (0.03)	0.30 (0.02)	39.42 (0.2)	55.45 (0.46)	0.69 (0.02)	0.79 (0.01)
327	0.57 (0.02)	0.35 (0.01)	36.43 (0.2)	56.03 (0.35)	0.68 (0.06)	0.68 (0.02)
328	0.50 (0.03)	0.36 (0.02)	38.80 (0.25)	47.60 (0.39)	0.73 (0.05)	0.58 (0.01)
329	0.63 (0.03)	0.46 (0.03)	32.30 (0.22)	49.47 (0.54)	0.83 (0.13)	0.81 (0.16)
330	0.75 (0.04)	0.60 (0.03)	30.88 (0.23)	45.23 (0.61)	0.56 (0.17)	0.57 (0.12)
331	0.59 (0.02)	0.30 (0.01)	26.46 (0.15)	41.51 (0.27)	0.74 (0.02)	0.85 (0.01)
332	0.62 (0.03)	0.40 (0.02)	32.96 (0.21)	43.22 (0.52)	0.63 (0.03)	0.59 (0.08)
333	0.59 (0.02)	0.48 (0.01)	25.78 (0.13)	40.90 (0.34)	0.12 (0.17)	0.23 (0)
334	0.70 (0.01)	0.47 (0.01)	31.39 (0.09)	41.89 (0.17)	0.54 (0.03)	0.55 (0.02)
335	0.66 (0.01)	0.49 (0.01)	29.33 (0.06)	40.98 (0.13)	0.41 (0.05)	0.54 (0)
336	0.61 (0.02)	0.34 (0.01)	38.27 (0.22)	47.60 (0.41)	0.54 (0.09)	0.76 (0.04)
337	0.56 (0.03)	0.33 (0.01)	37.91 (0.21)	46.21 (0.38)	0.81 (0.03)	0.76 (0.12)
338	0.59 (0.02)	0.37 (0.01)	38.59 (0.17)	49.20 (0.36)	0.70 (0.03)	0.82 (0.04)
340	0.52 (0.03)	0.31 (0.02)	40.50 (0.29)	54.06 (0.52)	0.64 (0.06)	0.81 (0.04)
347	0.52 (0.04)	0.30 (0.02)	32.88 (0.31)	50.02 (0.6)	0.63 (0.01)	0.77 (0.16)
349	0.57 (0.03)	0.31 (0.02)	34.17 (0.21)	49.26 (0.44)	0.75 (0.03)	0.77 (0.03)
350	0.45 (0.04)	0.35 (0.02)	35.72 (0.38)	45.57 (0.55)	0.65 (0.14)	0.86 (0.18)

Table S2 continued. ^{15}N Relaxation data.

Backbone Amide	R_1(1/s) 500MHz	R_1(1/s) 800MHz	R_2(1/s) 500MHz	R_2(1/s) 800MHz	{^{1}H}-^{15}N NOE 500MHz	{^{1}H}-^{15}N NOE 800MHz
351	0.62 (0.02)	0.41 (0.01)	33.85 (0.16)	48.03 (0.29)	0.43 (0.06)	0.44 (0.08)
352	0.54 (0.02)	0.40 (0.01)	33.84 (0.15)	46.85 (0.24)	0.31 (0.02)	0.53 (0.03)
355	1.28 (0.03)	0.90 (0.01)	6.22 (0.07)	7.50 (0.12)	0.04 (0.1)	0.29 (0.04)
356	1.54 (0.02)	1.36 (0.01)	5.23 (0.05)	5.59 (0.08)	0.04 (0.16)	0.30 (0.01)
357	1.40 (0.02)	1.25 (0.01)	8.52 (0.06)	11.04 (0.09)	0.11 (0.01)	0.34 (0.03)
358	1.40 (0.06)	1.21 (0.03)	5.90 (0.13)	6.37 (0.21)	-0.26 (0.07)	0.41 (0.08)
359	1.20 (0.02)	1.12 (0.01)	9.02 (0.06)	10.03 (0.1)	0.16 (0.02)	0.41 (0.01)
360	1.28 (0.03)	0.90 (0.01)	6.22 (0.07)	5.43 (0.11)	-0.11 (0.05)	0.29 (0.04)
361	1.56 (0.01)	1.35 (0.01)	5.22 (0.03)	5.08 (0.05)	-0.04 (0.13)	0.27 (0.01)
362	1.38 (0.07)	1.31 (0.05)	4.62 (0.16)	5.85 (0.24)	0.08 (0.34)	0.36 (0.08)
363	0.92 (0.04)	0.69 (0.14)	30.87 (0.22)	14.19 (4.61)	0.39 (0.06)	-0.18 (0.41)
364	0.98 (0.01)	0.70 (0.01)	9.03 (0.06)	4.57 (0.07)	0.45 (0.16)	0.67 (0.02)
365	1.36 (0.01)	1.32 (0.01)	2.85 (0.04)	3.69 (0.05)	-0.59 (0.11)	0.07 (0.04)
367	1.13 (0)	1.40 (0)	1.49 (0.02)	2.30 (0.02)	-1.31 (0.01)	-0.43 (0.01)

Table S3. Model free extracted parameters. S^2 is the squared generalized order parameter. $S^2 = S^2_f * S^2_s$ (fast and slow components). τ_e is the internal correlation time. R_{ex} is the exchange contribution to the transverse relaxation rate. The optimized rotational correlation time (τ_c) was 31ns. Models are described in the main text, using BIC (Bayesian information criterion) for model selection (lowest BIC).

Backbone Amide	S^2	S^2_f	τ_e(ns)	R_{ex}(1/s)	model	BIC
10	0.96 (0.05)		0.26 (0.9)	1.90 (1.13)	4	8.97
11	0.97 (0.01)		0.65 (0.41)	5.02 (0.78)	4	10.65
12	0.84 (0.03)			9.46 (1.09)	3	39.12
13	0.92 (0.02)			8.00 (1)	3	7.30
14	0.97 (0.01)		0.88 (0.33)		2	19.61
15	0.97 (0.01)		0.29 (0.12)	1.72 (0.68)	4	6.25
16	0.95 (0.01)		0.79 (0.12)		2	21.75
18	0.93 (0.01)		0.62 (0.14)	4.27 (0.75)	4	7.62
19	0.88 (0.01)		1.11 (0.08)		2	56.78
20	0.94 (0.01)		0.60 (0.12)		2	6.78
21	0.97 (0.01)		0.40 (0.15)		2	5.58
22	0.89 (0.05)		0.02 (0.05)	5.10 (1.21)	4	15.18
23	0.85 (0.03)		0.01 (0)	3.54 (0.86)	4	13.49
25	0.92 (0.02)	0.94 (0.02)	0.92 (0.6)		5	16.74
26	0.91 (0.03)		0.02 (0.01)	2.76 (0.95)	4	6.53
27	0.99 (0.01)		1.10 (3.78)		2	7.58
28	0.93 (0.02)		0.04 (0.03)		2	15.48
29	0.85 (0.02)		0.02 (0.01)	7.48 (0.99)	4	31.78
30	0.86 (0.03)		0.01 (0)	8.77 (1.01)	4	8.80
31	0.87 (0.02)				1	73.94
36	0.93 (0.01)		0.38 (0.06)		2	11.55
38	0.88 (0.03)	0.94 (0.02)	2.05 (0.95)		5	42.52
42	0.94 (0.04)		0.04 (0.15)	3.67 (1.12)	4	13.05
43	0.98 (0.01)		0.15 (0.19)		2	7.21
45	0.88 (0.03)			4.41 (0.98)	3	13.97
46	0.89 (0.02)		0.02 (0.01)	5.82 (1.01)	4	7.99
47	0.98 (0.01)		0.71 (0.23)		2	12.13
48	0.98 (0.01)		0.17 (0.16)		2	7.49
50	0.76 (0.05)		0.02 (0.01)	2.77 (1.34)	4	12.92
51	0.91 (0.03)		0.04 (0.02)	5.06 (1.01)	4	17.79
52	0.93 (0.01)		0.47 (0.06)		2	36.31
57	0.93 (0.03)			3.68 (1.03)	3	12.58
58	0.97 (0.02)		0.06 (0.24)		2	10.17
59	0.87 (0.03)		0.03 (0.01)	2.92 (0.93)	4	13.64
60	0.90 (0.05)			5.79 (1.3)	3	8.19
62	0.96 (0.02)				1	23.29
63	0.89 (0.04)		0.01 (0.02)	7.25 (1.3)	4	23.73
68	0.72 (0.1)		35.90 (15.86)		2	11.15
69	0.98 (0.01)		1.01 (0.48)		2	10.24
70	0.85 (0.03)	0.91 (0.03)	1.32 (0.44)		5	6.80
83	0.87 (0.01)		1.01 (0.06)		2	47.34
84	0.96 (0.02)				1	23.23
85	0.91 (0.02)				1	6.51

Table S3 continued. Model free extracted parameters.

Backbone Amide	S^2	S^2_f	τ_e(ns)	R_{ex}(1/s)	model	BIC
86	0.98 (0.01)		0.69 (0.28)		2	24.37
87	0.91 (0.05)		0.02 (0.11)	4.91 (1.44)	4	13.91
88	0.95 (0.01)		0.83 (0.21)		2	16.47
89	0.97 (0.01)		0.44 (0.15)		2	13.23
90	0.88 (0.06)		16.38 (12.49)		2	4.16
94	1.00 (0.01)				1	13.68
96	0.65 (0.02)	0.69 (0.02)	0.92 (0.19)		5	41.75
97	0.86 (0.02)	0.94 (0.02)	0.95 (0.13)		5	8.46
98	0.93 (0.01)		0.54 (0.07)		2	11.31
100	0.98 (0.01)		0.69 (0.24)	5.19 (0.9)	4	13.87
101	0.87 (0.02)		0.04 (0.01)		2	15.81
102	0.82 (0.03)		0.03 (0.01)	4.07 (1.07)	4	14.12
103	0.64 (0.06)		0.01 (0)	7.14 (1.75)	4	10.57
111	0.95 (0.01)		0.88 (0.25)		2	41.18
112	0.55 (0.05)		15.51 (3.23)		2	7.54
114	0.84 (0.02)	0.91 (0.02)	1.54 (0.53)		5	6.86
115	0.95 (0.01)		0.74 (0.13)		2	9.25
116	0.91 (0.03)			4.00 (1.01)	3	7.44
118	0.83 (0.04)		0.01 (0)	5.67 (1.12)	4	10.43
120	0.92 (0.01)		1.05 (0.11)		2	19.92
121	0.95 (0.01)		0.25 (0.09)	2.36 (0.67)	4	17.58
122	0.89 (0.01)		0.52 (0.05)		2	7.81
123	0.77 (0.02)	0.92 (0.02)	1.01 (0.07)		5	13.45
125	0.83 (0.01)		0.69 (0.04)		2	17.41
126	0.96 (0.01)		0.93 (0.15)	1.34 (0.61)	4	15.46
127	0.96 (0.01)		0.92 (0.24)		2	16.74
130	0.82 (0.02)	0.87 (0.02)	1.80 (0.62)		5	26.25
131	0.95 (0.02)				1	5.59
132	0.89 (0.03)		0.02 (0.01)	5.72 (0.95)	4	11.41
133	0.78 (0.02)	0.91 (0.02)	1.01 (0.07)		5	12.22
135	0.95 (0.08)		3.92 (8.8)	1.56 (1.07)	4	9.76
147	0.91 (0.03)		0.04 (0.19)		2	9.77
148	0.99 (0.01)		0.10 (0.26)		2	16.23
158	0.97 (0.01)		0.62 (1.57)		2	22.92
159	0.62 (0.05)		0.00 (0)	8.21 (1.51)	4	26.75
161	0.89 (0.04)		0.02 (0.01)	2.53 (1.03)	4	16.43
162	0.93 (0.02)		0.01 (0.01)		2	30.28
163	0.94 (0.01)		0.34 (0.09)	3.41 (0.69)	4	25.43
164	0.91 (0.02)		0.06 (0.02)		2	11.59
165	0.98 (0.03)		0.31 (0.22)	2.32 (0.92)	4	21.87
166	0.89 (0.03)		0.01 (0.01)	5.52 (0.88)	4	28.93
167	0.96 (0.02)		0.06 (0.17)		2	6.62
168	0.97 (0.02)		0.11 (0.37)		2	44.13
172	0.91 (0.01)		0.89 (0.07)		2	43.78
173	0.63 (0.09)		0.01 (0.01)	10.73 (2.54)	4	7.59

Table S3 continued. Model free extracted parameters.

Backbone Amide	S^2	S^2_f	τ_e(ns)	R_{ex}(1/s)	model	BIC
175	0.87 (0.01)		1.29 (0.1)		2	35.15
176	0.88 (0.01)		0.64 (0.04)		2	19.27
179	0.88 (0.02)		1.26 (0.35)		2	10.65
181	0.54 (0.02)	0.70 (0.02)	2.30 (0.29)		5	21.56
182	0.55 (0.02)	0.73 (0.02)	1.67 (0.13)		5	11.36
185	0.89 (0.02)				1	102.91
186	0.76 (0.02)		1.40 (0.14)	1.49 (0.61)	4	9.70
206	0.64 (0.06)			6.72 (1.48)	3	8.25
209	0.88 (0.05)		0.02 (0.03)	5.92 (1.28)	4	5.99
212	0.88 (0.02)		0.03 (0.01)		2	16.93
217	0.97 (0.02)			2.14 (0.85)	3	10.24
220	0.93 (0.03)		0.04 (0.04)	5.73 (1.03)	4	21.18
221	0.71 (0.04)		0.01 (0)	2.39 (1.06)	4	19.82
222	0.95 (0.01)		0.72 (0.11)		2	6.37
223	0.90 (0.02)				1	47.60
224	0.86 (0.02)	0.90 (0.02)	1.43 (0.58)		5	8.75
233	0.90 (0.05)			4.29 (1.36)	3	4.51
234	0.94 (0.02)		1.70 (0.94)		2	9.57
241	0.98 (0.01)		0.34 (0.17)	3.76 (0.8)	4	9.56
243	0.97 (0.01)		0.32 (0.28)		2	9.15
247	0.90 (0.03)		0.06 (0.04)	8.43 (1.13)	4	6.44
248	0.91 (0.01)		0.71 (0.14)		2	13.57
249	0.78 (0.06)		0.02 (0.01)	4.00 (1.5)	4	12.52
251	0.84 (0.03)		0.03 (0.01)	-0.05 (0.68)	4	18.83
252	0.80 (0.02)	0.86 (0.02)	0.96 (0.14)		5	32.59
253	0.85 (0.05)			6.02 (1.24)	3	6.78
259	0.98 (0.01)		0.36 (0.27)		2	4.96
260	0.97 (0.01)		1.07 (0.27)		2	8.09
261	0.97 (0.01)		0.27 (0.12)		2	24.78
262	0.93 (0.01)		1.55 (0.33)		2	23.12
263	0.95 (0.01)		0.66 (0.12)		2	6.34
264	0.96 (0.01)		0.43 (0.21)		2	11.70
265	0.92 (0.01)		0.66 (0.08)		2	10.12
267	0.89 (0.01)		0.56 (0.05)		2	17.11
268	0.81 (0.02)	0.93 (0.02)	1.27 (0.21)		5	6.26
269	0.82 (0.02)	0.96 (0.02)	0.87 (0.06)		5	15.61
270	0.88 (0.01)		0.79 (0.05)		2	23.55
271	0.93 (0.01)		0.68 (0.07)		2	4.26
273	0.94 (0.01)		0.54 (0.16)	3.51 (0.79)	4	8.40
274	0.86 (0.03)		0.04 (0.01)	-0.06 (0.6)	4	20.98
275	0.90 (0.02)	0.95 (0.02)	0.56 (0.12)		5	7.54
277	0.88 (0.03)		0.03 (0.01)	2.21 (0.92)	4	13.88
279	0.90 (0.01)		0.40 (0.05)		2	17.61
280	0.93 (0.01)		0.24 (0.05)		2	17.52
281	0.87 (0.02)		0.07 (0.02)	4.75 (0.93)	4	15.93

Table S3 continued. Model free extracted parameters.

Backbone Amide	S^2	S^2_f	τ_e(ns)	R_{ex}(1/s)	model	BIC
283	0.92 (0.01)		1.03 (0.1)		2	16.77
284	0.96 (0.02)				1	3.61
285	0.89 (0.02)				1	19.53
286	0.96 (0.01)		1.76 (1.44)		2	21.29
287	0.87 (0.03)	0.91 (0.02)	1.69 (0.83)		5	11.54
288	0.71 (0.03)	0.84 (0.03)	1.50 (0.26)		5	32.75
294	0.96 (0.04)			9.24 (1.2)	3	8.60
295	0.97 (0.02)		0.08 (0.17)		2	8.10
298	0.96 (0.01)		1.81 (1.05)		2	21.44
299	0.67 (0.11)		49.16 (20.33)		2	16.69
300	0.97 (0.01)		0.32 (0.14)		2	42.28
301	0.87 (0.04)		0.03 (0.01)	4.30 (1.35)	4	8.39
303	0.89 (0.02)		0.02 (0.01)		2	4.28
304	0.96 (0.01)		0.61 (0.14)		2	9.17
306	0.93 (0.03)			4.84 (1.08)	3	21.69
307	0.81 (0.03)	0.92 (0.02)	1.10 (0.16)		5	9.18
310	0.93 (0.06)		28.76 (22.56)		2	6.63
312	0.86 (0.03)		0.03 (0.01)	7.88 (1.04)	4	12.95
313	0.93 (0.01)		0.83 (0.11)		2	10.30
315	0.94 (0.03)		0.03 (0.03)	5.64 (0.96)	4	20.91
316	0.54 (0.01)		1.00 (0.03)		2	100.98
318	0.48 (0.02)	0.83 (0.02)	1.15 (0.06)		5	17.75
319	0.50 (0.02)	0.84 (0.02)	1.15 (0.05)		5	25.96
320	0.51 (0.01)		1.01 (0.03)		2	157.25
322	0.63 (0.01)		1.03 (0.03)		2	168.11
323	0.76 (0.02)	0.94 (0.02)	0.61 (0.03)		5	37.54
324	0.88 (0.01)		0.77 (0.05)		2	27.76
325	0.88 (0.02)	0.95 (0.02)	0.54 (0.09)		5	11.89
326	0.90 (0.03)		0.02 (0.01)	5.86 (0.95)	4	9.69
327	0.97 (0.01)		0.40 (0.14)	3.07 (0.73)	4	9.25
328	0.52 (0.02)		0.02 (0)	-0.09 (0.53)	4	23.04
329	0.91 (0.01)		1.49 (0.45)		2	20.28
330	0.73 (0.02)	0.91 (0.02)	1.38 (0.27)		5	9.03
331	0.85 (0.02)				1	52.03
332	0.93 (0.01)		1.03 (0.12)		2	21.32
333	0.65 (0.02)	0.84 (0.02)	0.64 (0.03)		5	16.66
334	0.91 (0.01)		0.85 (0.07)		2	10.31
335	0.89 (0.01)		0.73 (0.06)		2	10.45
336	0.97 (0.01)		0.53 (0.19)		2	8.85
337	0.86 (0.02)	0.91 (0.02)	3.49 (1.86)		5	8.05
338	0.96 (0.01)		1.27 (0.31)		2	5.52
340	0.96 (0.01)		0.99 (0.21)		2	5.46
347	0.87 (0.02)		0.03 (0.01)		2	22.60
349	0.94 (0.02)	0.96 (0.02)	0.83 (0.31)		5	7.37
350	0.90 (0.03)	0.93 (0.03)	0.96 (0.9)		5	13.82

Table S4. Methyl relaxation dispersion individually fitted parameters (283K)

Methyl	R_{20}(1/s) 500MHz		R_{20}(1/s) 800MHz		R_{ex}(1/s) 800MHz	k_{ex}(1/s)		$\Delta\omega_C$ (ppm)	$p_{B(\%)}$	model	$\frac{\chi^2(0)}{\chi^2(ex)}$	$\frac{\chi^2(\Delta\omega H0)}{\chi^2(\Delta\omega H)}$
Met1-ε	2.1	(0.3)	1.6	(0.8)						0	1.3	
Val16-γ1	18.3	(0.5)	23.1	(3.5)						0	0.9	
Val16-γ2	19.5	(0.4)	24.4	(0.6)						0	2.7	
Val23-γ1	19.1	(0.6)	25.2	(0.7)						0	1.0	
Val23-γ2	20.7	(118.5)	27.4	(193.9)						0	0.9	
Val26-γ1	13.6	(0.4)	20.2	(1.8)						0	1.0	
Val26-γ2	15.7	(13.1)	20.5	(24.4)						0	2.4	
Leu30-δ1	24.3	(0.2)	25.4	(0.1)						0	1.0	
Leu30-δ2	23.1	(0.1)	26.6	(0.1)						0	1.9	
Val33-γ1	9.8	(1.7)	6.8	(3.1)						0	1.2	
Val41-γ1	16.3	(58.6)	17.1	(96)						0	0.9	
Val45-γ1	22.9	(0.2)	22.1	(0.1)						0	1.3	
Val45-γ2	20.6	(0.3)	22.5	(0.2)						0	1.1	
Val53-γ1	26.0	(0.6)	26.1	(0.4)						0	1.0	
Val53-γ2	31.3	(0.5)	35.7	(0.4)						0	1.2	
Ile55-δ	26.3	(0.3)	30.1	(0.4)						0	0.9	
Leu58-δ1	23.1	(0.1)	26.6	(0.1)						0	1.9	
Leu58-δ2	27.3	(0.5)	28.2	(0.4)						0	2.1	
Leu66-δ2	21.5	(0.2)	21.6	(0.2)						0	1.7	
Leu75-δ1	11.5	(0.4)	13.9	(912.3)						0	0.9	
Leu75-δ2	13.0	(0.4)	13.2	(0.5)						0	0.9	
Leu77-δ1	49.7	(2)	76.6	(2.1)	25.1	826	(387)			1	4.7	1.0
Met81-ε	67.7	(2)	92.3	(1.9)						0	1.2	
Val86-γ2	18.5	(0.1)	23.0	(0.1)	3.3	1321	(154)			1	5.7	1.0
Ile87-δ	38.8	(0.3)	42.3	(0.3)	5.9	1371	(281)			1	12.2	1.0
Leu89-d2	36.4	(0.5)	41.3	(0.5)						0	1.3	
Leu90-δ1	19.3	(0.3)	17.2	(0.2)						0	1.2	
Leu90-δ2	10.6	(0.1)	13.1	(0.1)						0	3.0	
Val92-γ1	2.2	(0.2)	2.1	(0.2)						0	1.5	
Leu107-δ1	13.6	(0.1)	17.1	(1.7)						0	0.9	
Leu107-δ2	23.6	(0.1)	27.1	(0.1)						0	1.4	
Met112-ε	42.3	(1.1)	49.3	(1.4)						0	0.9	
Leu116-δ1	9.2	(1.6)	11.1	(1.7)						0	1.2	
Leu116-δ2	31.3	(0.5)	38.9	(0.5)						0	1.3	
Leu119-δ1	24.3	(0.2)	25.4	(0.1)						0	1.0	
Leu119-δ2	23.1	(0.1)	26.6	(0.1)						0	1.8	
Met120-ε	34.3	(0.2)	37.6	(0.1)	3.7	641	(169)			1	4.7	1.0

$\chi^2(0)/\chi^2(ex)$ is the ratio of the χ^2 for a flat line over the χ^2 for fitted 2-site exchange:
An F-critical value of 3.46 corresponds to a 99.99% confidence level.
$\chi^2(\Delta\omega H0)/\chi^2(\Delta\omega H)$ is the ratio of the χ^2 for a fit with fixed $\Delta\omega H=0$ over the χ^2 for a fit with varying $\Delta\omega H$:
An F-critical value of 1.94 corresponds to a 95% confidence level.
Model 1(2): fast (general) 2-site exchange.

Table S4 continued. Methyl relaxation dispersion individually fitted parameters (283K)

Methyl	R_{20}(1/s) 500MHz		R_{20}(1/s) 800MHz		R_{ex}(1/s) 800MHz	k_{ex}(1/s)		$\Delta\omega_C$ (ppm)	$p_{B(\%)}$	model	$\frac{\chi^2(0)}{\chi^2(ex)}$	$\frac{\chi^2(\Delta\omega H0)}{\chi^2(\Delta\omega H)}$
Leu125-δ1	56.6	(0.5)	71.7	(0.4)						0	1.1	
Ile130-δ	36.6	(0.2)	37.2	(0.2)						0	0.9	
Leu133-δ2	29.8	(0.7)	26.9	(0.8)						0	1.1	
Met137-ε	46.2	(0.4)	50.0	(0.4)	7.2	1464	(340)			1	13.4	1.0
Ile144-δ	45.4	(1.3)	68.8	(163.5)						0	0.9	
Ile149-δ	36.4	(0.4)	56.3	(0.4)	64.0	1047	(41)			1	67.2	1.0
Ile150-δ	21.3	(0.1)	29.3	(0.1)	10.1	889	(56)			1	27.3	1.0
Leu159-δ1	67.2	(129.1)	67.7	(211.2)						0	0.9	
Val161-γ1	26.0	(0.6)	26.1	(0.4)						0	1.0	
Val161-γ2	25.7	(0.6)	27.7	(0.6)						0	1.3	
Leu167-δ1	64.8	(3.5)	65.3	(302.2)						0	0.9	
Leu167-δ2	25.0	(0.7)	30.6	(0.7)						0	1.3	
Ile169-δ	30.3	(0.2)	44.3	(0.3)						0	2.8	
Met182-ε	18.3	(0.1)	26.7	(0.1)	28.8	686	(12)	0.84(0.01)	3.1	2	101.9	1.0
Val186-γ1	19.4	(0.3)	27.4	(0.3)						0	1.9	
Val186-γ2	14.2	(0.1)	17.5	(0.1)						0	3.1	
Val187-γ	19.4	(0.2)	27.4	(0.3)						0	1.9	
Val187-γ	14.2	(0)	17.5	(0.1)						0	3.1	
Ile197-δ	37.8	(0.3)	37.2	(0.2)						0	0.9	
Ile209-δ	33.5	(0.3)	43.8	(0.3)	37.4	1224	(54)			1	55.1	1.0
Val212-γ1	15.3	(2)	19.7	(28.5)						0	1.0	
Val212-γ2	57.6	(3.3)	71.1	(3.8)						0	1.0	
Ile215-δ	31.7	(0.3)	39.1	(0.3)						0	1.6	
Met219-ε	44.9	(0.3)	47.6	(0.2)	6.6	768	(175)			1	9.1	1.1
Ile220-δ	45.0	(0.4)	50.1	(1.6)						0	1.0	
Leu225-δ1	26.2	(0.6)	37.3	(0.7)	238.3	771	(34)			1	146.1	1.0
Leu225-δ2	46.1	(5.1)	84.5	(5.6)	325.9	1111	(267)			1	18.8	1.0
Leu232-δ2	36.7	(0.7)	44.5	(0.9)						0	1.1	
Ile238-δ	22.6	(0.2)	24.5	(0.2)						0	1.2	
Val241-γ1	33.3	(0.3)	43.3	(0.3)						0	1.2	
Val241-γ2	32.8	(0.3)	40.6	(0.3)						0	1.4	
Val250-γ1	16.1	(0.1)	19.8	(2.6)						0	1.0	
Val250-γ2	32.8	(0.3)	40.6	(0.3)						0	1.4	
Leu253-δ2	13.9	(0.1)	17.0	(0.1)						0	0.9	
Met262-ε	33.4	(0.2)	44.3	(0.2)	39.3	563	(39)	0.77(0.03)	4.9	2	121.8	1.0
Leu265-δ1	52.7	(1.1)	71.3	(1.1)						0	1.9	
Leu268-δ(2)	35.2	(0.3)	42.5	(0.3)						0	1.0	

$\chi^2(0)/\chi^2(ex)$ is the ratio of the χ^2 for a flat line over the χ^2 for fitted 2-site exchange:
An F-critical value of 3.46 corresponds to a 99.99% confidence level.
$\chi^2(\Delta\omega H0)/\chi^2(\Delta\omega H)$ is the ratio of the χ^2 for a fit with fixed $\Delta\omega H=0$ over the χ^2 for a fit with varying $\Delta\omega H$:
An F-critical value of 1.94 corresponds to a 95% confidence level.
Model 1(2): fast (general) 2-site exchange.

Table S4 continued. Methyl relaxation dispersion individually fitted parameters (283K)

Methyl	R_{20}(1/s) 500MHz		R_{20}(1/s) 800MHz		R_{ex}(1/s) 800MHz	k_{ex}(1/s)		$\Delta\omega_C$ (ppm)	$p_{B(\%)}$	model	$\frac{\chi^2(0)}{\chi^2(ex)}$	$\frac{\chi^2(\Delta\omega H0)}{\chi^2(\Delta\omega H)}$
Leu268-δ	25.9	(1.2)	39.6	(1.2)						0	1.7	
Ile276-δ	22.6	(0.2)	24.5	(0.2)						0	1.2	
Leu277-δ1	32.4	(0.5)	41.6	(0.4)						0	0.9	
Leu277-δ2	29.4	(0.4)	36.0	(0.3)						0	1.3	
Leu283-δ1	31.3	(0.5)	38.9	(0.5)						0	1.3	
Leu283-δ2	25.3	(0.3)	32.5	(0.3)						0	1.0	
Val285-γ1	16.6	(0.3)	20.8	(1.5)						0	1.0	
Val285-γ2	16.8	(0.3)	20.4	(0.2)						0	1.7	
Leu287-δ1	33.3	(0.3)	43.3	(0.3)						0	1.2	
Leu287-δ2	42.8	(0.8)	53.6	(0.8)						0	0.9	
Leu288-δ1	42.1	(1.1)	63.8	(1.1)	34.2	792	(165)			1	8.2	1.0
Leu288-δ2	26.7	(0.4)	36.6	(0.4)	19.8	751	(104)			1	26.9	1.0
Met291-ε	36.5	(0.2)	38.5	(0.1)	7.3	569	(87)			1	6.9	1.1
Leu292-δ1	51.0	(1.2)	62.4	(1.2)	17.6	1029	(369)			1	11.9	1.0
Leu292-δ2	36.3	(0.4)	41.0	(0.4)						0	2.1	
Val293-γ1	15.9	(0.2)	22.2	(0.2)	3.1	1097	(305)			1	4.9	1.0
Val293-γ2	15.0	(1.4)	19.4	(1.6)						0	1.1	
Leu294-δ1	25.8	(0.3)	41.8	(0.3)						0	1.5	
Leu294-δ2	51.5	(3.2)	60.3	(3.5)	98.0	1180	(212)			1	7.6	1.0
Val300-γ1	14.1	(0.6)	11.3	(0.6)						0	2.4	
Val300-γ2	19.4	(0.3)	27.4	(0.3)						0	1.9	
Leu314-δ2	16.4	(0.3)	16.9	(0.3)						0	1.1	
Val323-γ1	20.4	(0.6)	27.8	(0.9)	4.3	3758	(1808)			1	6.0	1.0
Val323-γ2	32.8	(0.3)	40.6	(0.3)						0	1.4	
Val333-γ2	14.2	(0.1)	17.5	(0.1)						0	3.1	
Leu337-δ1	16.8	(0.3)	20.4	(0.2)						0	1.7	
Leu337-δ2	11.6	(1)	0.6	(1.1)						0	2.0	
Val343-γ1	24.4	(0.3)	25.2	(0.2)						0	1.0	
Val343-γ2	17.1	(1.3)	20.6	(1.2)						0	1.7	
Val348-γ2	15.9	(0.4)	17.2	(5.5)						0	0.9	
Leu357-δ1	5.0	(0.4)	3.8	(0.2)						0	1.3	
Leu357-δ2	9.1	(0.6)	7.0	(1.1)						0	1.0	
Val361-γ1	9.0	(0.1)	8.6	(0.2)						0	3.2	
Val361-γ2	3.4	(0.1)	2.1	(0.2)						0	2.8	
Leu367-δ1	8.1	(0.1)	10.0	(0.1)						0	1.6	
Leu367-δ2	8.4	(0.1)	7.7	(0.1)						0	3.4	

$\chi^2(0)/\chi^2(ex)$ is the ratio of the χ^2 for a flat line over the χ^2 for fitted 2-site exchange:
An F-critical value of 3.46 corresponds to a 99.99% confidence level.
$\chi^2(\Delta\omega H0)/\chi^2(\Delta\omega H)$ is the ratio of the χ^2 for a fit with fixed $\Delta\omega H=0$ over the χ^2 for a fit with varying $\Delta\omega H$:
An F-critical value of 1.94 corresponds to a 95% confidence level.
Model 1(2): fast (general) 2-site exchange.

Table S5. Methyl relaxation dispersion fitted individually fit parameters (293K)

Methyl	R_{20}(1/s) 500MHz		R_{20}(1/s) 800MHz		R_{ex}(1/s) 800MHz	k_{ex}(1/s)		$\Delta\omega_C$ (ppm)	$p_{B(\%)}$	model	$\frac{\chi^2(0)}{\chi^2(ex)}$	$\frac{\chi^2(\Delta\omega H0)}{\chi^2(\Delta\omega H)}$
Met1-ε	2.0	(0.1)	1.4	(0.1)						0	1.2	
Val16-γ1	13.5	(23.2)	15.1	(36.2)						0	1.1	
Val16-γ2	12.8	(23.7)	15.2	(37)						0	3.4	
Val23-γ1	20.1	(0.1)	24.4	(0.2)						0	1.1	
Val23-γ2	17.3	(0.7)	19.6	(1)						0	2.4	
Val26-γ1	9.7	(17.8)	12.3	(27.8)						0	1.1	
Val26-γ2	10.9	(0.2)	14.1	(0.2)						0	3.2	
Leu30-δ1	17.7	(0.1)	16.6	(0.2)						0	1.7	
Val33-γ1	9.1	(0.4)	4.7	(0.9)						0	1.9	
Val41-γ1	10.6	(0.1)	12.2	(0.1)						0	1.0	
Val45-γ1	14.6	(0.1)	15.6	(0.1)						0	1.3	
Val45-γ2	12.7	(0.1)	15.9	(0.1)						0	1.3	
Val53-γ1	18.4	(0.1)	16.9	(0.1)						0	1.8	
Val53-γ2	22.9	(0.3)	25.4	(0.4)						0	1.2	
Ile55-δ	18.9	(11.5)	20.9	(17.9)						0	0.9	
Leu58-δ1	15.7	(0.2)	17.2	(0.3)						0	1.2	
Leu58-δ2	20.1	(0.2)	20.3	(0.2)						0	3.4	
Leu66-δ2	13.3	(0.1)	16.1	(0.1)						0	1.0	
Leu75-δ1	10.4	(14)	10.8	(21.9)						0	0.9	
Leu75-δ2	9.8	(0.1)	8.8	(0.2)	1.8					1	4.3	
Leu77-δ1	35.2	(1)	52.5	(1.6)	9.0	2334	(1498)			1	5.6	1.0
Met81-ε	35.5	(71.8)	44.0	(112.2)						0	2.9	
Val86-γ2	13.1	(0.2)	15.5	(0.3)						0	1.8	
Ile87-δ	28.1	(0.2)	30.4	(0.3)	3.6	3010	(774)			1	6.1	1.0
Leu89-d2	27.0	(0.3)	30.1	(0.4)						0	1.6	
Leu90-δ1	21.3	(0.1)	20.4	(0.2)						0	1.6	
Leu90-δ2	8.2	(0.1)	9.9	(0.2)						0	3.5	
Val92-γ1	2.5	(0.1)	1.1	(0.2)						0	2.3	
Leu107-δ1	10.9	(0.1)	11.6	(0.1)						0	1.2	
Leu107-δ2	15.7	(0)	17.5	(0.1)						0	2.1	
Met109-ε	11.3	(0.3)	9.3	(0.7)	20.3	2749	(228)			1	17.6	1.0
Met112-ε	28.5	(0.1)	32.3	(0.2)	2.6	830	(297)			1	5.8	1.0
Leu116-δ1	6.5	(0)	7.3	(0.1)						0	1.9	
Leu116-δ2	25.9	(0.2)	27.6	(0.4)						0	1.3	
Leu119-δ1	17.7	(0.1)	16.6	(0.2)						0	1.7	
Leu119-δ2	18.4	(0.1)	19.3	(0.1)	3.1	1202	(238)			1	6.7	1.0
Met120-ε	24.3	(0.1)	25.1	(0.1)	2.7	983	(168)			1	10.7	1.0

$\chi^2(0)/\chi^2(ex)$ is the ratio of the χ^2 for a flat line over the χ^2 for fitted general 2-site exchange:
An F-critical value of 3.77 corresponds to a 99.99% confidence level.
$\chi^2(\Delta\omega H0)/\chi^2(\Delta\omega H)$ is the ratio of the χ^2 for a fit with fixed $\Delta\omega H=0$ over the χ^2 for a fit with varying $\Delta\omega H$:
An F-critical value of 2.03 corresponds to a 95% confidence level.
Model 1(2): fast (general) 2-site exchange.

Table S5 continued. Methyl relaxation dispersion individually fit parameters (293K)

Methyl	R_{20}(1/s) 500MHz		R_{20}(1/s) 800MHz		R_{ex}(1/s) 800MHz	k_{ex}(1/s)		$\Delta\omega_C$ (ppm)		$p_{B(\%)}$	model	$\frac{\chi^2(0)}{\chi^2(ex)}$	$\frac{\chi^2(\Delta\omega H0)}{\chi^2(\Delta\omega H)}$
Leu125-δ1	29.9	(22)	35.2	(34.3)							0	0.9	
Ile130-δ	26.1	(0.1)	26.9	(0.2)							0	0.9	
Leu133-δ2	25.9	(0.2)	27.6	(0.4)							0	1.3	
Met137-ε	32.2	(0.2)	34.4	(0.2)	3.4	1675	(413)				1	32.2	1.0
Ile144-δ	32.0	(41.3)	43.9	(64.6)							0	0.9	
Ile149-δ	24.5	(0.2)	34.9	(0.3)	20.7	2500	(135)				1	160.3	1.0
Ile150-δ	14.3	(0)	18.0	(0.1)	2.1						1	6.8	
Leu159-δ1	42.6	(0.3)	48.6	(0.4)							0	0.9	
Val161-γ1	18.4	(0.1)	16.9	(0.1)							0	1.8	
Val161-γ2	17.5	(0.2)	17.6	(0.3)							0	2.6	
Leu167-δ1	42.1	(59.7)	47.8	(93.3)							0	0.9	
Leu167-δ2	18.4	(0.1)	19.4	(0.1)	3.0	1149	(235)				1	7.4	1.0
Ile169-δ	14.2	(0)	17.9	(0.1)	2.2						1	6.7	
Met182-ε	9.0	(0.6)	11.3	(1.3)	11.4	2120	(480)	2.22	(0.2)	1	2	42.1	1.8
Val186-γ1	12.5	(0.1)	12.8	(0.4)							0	2.0	
Val186-γ2	9.7	(0.1)	10.9	(0.1)	4.8	2079	(159)				1	20.6	1.0
Val187-γ	12.5	(0.1)	12.8	(0.4)							0	2.0	
Val187-γ	9.7	(0.1)	10.9	(0.1)	4.8	2079	(159)				1	20.6	1.0
Ile197-δ	27.3	(0.1)	26.9	(0.2)							0	0.9	
Ile209-δ	22.6	(0.1)	27.0	(0.2)	13.5	2440	(142)				1	106.5	1.0
Val212-γ1	33.3	(0.4)	35.9	(0.6)							0	1.0	
Val212-γ2	46.3	(173.7)	51.9	(271.4)							0	0.9	
Ile215-δ	22.4	(0.1)	26.6	(0.2)							0	1.4	
Met219-ε	31.8	(0.1)	32.1	(0.2)	5.0	979	(134)				1	17.9	1.2
Ile220-δ	32.5	(29)	34.4	(45.3)							0	1.0	
Leu225-δ1	20.9	(0.4)	27.1	(0.6)	82.4	2165	(80)				1	204.3	1.0
Leu225-δ2	31.2	(2)	42.9	(3.3)	190.5	2398	(238)				1	79.5	1.0
Leu232-δ2	26.9	(0.2)	31.5	(0.3)							0	1.0	
Ile238-δ	18.6	(0)	18.7	(0.1)	1.3						1	3.8	
Val241-γ1	25.9	(0.2)	27.1	(0.3)							0	1.9	
Val241-γ2	22.5	(0.1)	26.9	(0.2)							0	2.5	
Val250-γ1	11.9	(0.1)	14.7	(0.1)							0	1.4	
Val250-γ2	22.8	(0.1)	27.0	(0.2)							0	2.3	
Leu253-δ2	9.6	(0.1)	10.7	(0.1)							0	2.7	
Met262-ε	19.5	(0.1)	26.6	(0.1)	15.5	1744	(52)				1	92.2	1.0
Leu265-δ1	38.0	(0.4)	44.4	(0.5)	5.1	1894	(777)				1	5.2	1.0
Leu268-δ(2)	24.5	(0.2)	28.2	(0.4)							0	1.5	
Leu268-δ	29.2	(0.7)	32.5	(1)							0	3.0	
Ile276-δ	18.6	(0)	18.7	(0.1)	1.3						1	3.8	
Leu277-δ1	23.5	(0.8)	24.7	(1.3)							0	1.2	

$\chi^2(0)/\chi^2(ex)$ is the ratio of the χ^2 for a flat line over the χ^2 for fitted general 2-site exchange:
An F-critical value of 3.77 corresponds to a 99.99% confidence level.
$X^2(\Delta\omega H0)/\chi^2(\Delta\omega H)$ is the ratio of the χ^2 for a fit with fixed $\Delta\omega H=0$ over the χ^2 for a fit with varying $\Delta\omega H$:
An F-critical value of 2.03 corresponds to a 95% confidence level.
Model 1(2): fast (general) 2-site exchange.

Table S5 continued. Methyl relaxation dispersion individually fit parameters (293K)

Methyl	R_{20}(1/s) 500MHz		R_{20}(1/s) 800MHz		R_{ex}(1/s) 800MHz	k_{ex}(1/s)		$\Delta\omega_C$ (ppm)	$p_{B(\%)}$	model	$\frac{\chi^2(0)}{\chi^2(ex)}$	$\frac{\chi^2(\Delta\omega H0)}{\chi^2(\Delta\omega H)}$
Leu277-δ2	20.0	(0.1)	22.9	(0.2)						0	1.3	
Leu283-δ1	25.9	(0.2)	27.6	(0.4)						0	1.3	
Leu283-δ2	17.7	(0.2)	21.6	(0.2)						0	1.1	
Val285-γ1	13.4	(0.1)	13.9	(0.2)						0	0.9	
Val285-γ2	12.3	(0)	14.2	(0.1)	1.5					1	4.7	
Leu287-δ1	27.5	(0.2)	28.9	(0.3)						0	1.6	
Leu287-δ2	32.8	(63.4)	38.7	(99)						0	0.9	
Leu288-δ1	27.7	(0.4)	35.9	(0.7)	11.2	2464	(517)			1	21.5	1.0
Leu288-δ2	18.8	(0.2)	24.8	(0.3)	3.6	2006	(668)			1	3.8	1.0
Met291-ε	25.9	(0.1)	26.0	(0.1)	4.6	1135	(134)			1	22.9	0.8
Leu292-δ1	35.8	(0.6)	40.9	(0.9)	10.5	2179	(677)			1	23.7	1.0
Leu292-δ2	27.7	(0.3)	29.4	(0.4)						0	2.2	
Val293-γ1	9.6	(0.1)	11.4	(0.1)	1.8					1	5.4	
Val293-γ2	9.2	(0.5)	9.3	(0.8)						0	3.5	
Leu294-δ1	14.6	(0.1)	22.0	(0.1)						0	1.0	
Leu294-δ2	30.7	(1.2)	53.7	(2)	24.7	3019	(771)			1	16.0	1.0
Val300-γ1	9.1	(0.2)	9.3	(0.4)	5.0	1422	(369)			1	4.4	1.0
Val300-γ2	12.5	(0.1)	12.8	(0.4)						0	2.0	
Leu314-δ2	15.5	(0.2)	15.0	(0.5)	6.3	1351	(292)			1	5.7	1.3
Val323-γ1	14.7	(0.3)	18.8	(0.4)	2.4	3334	(1559)			1	4.3	1.0
Val323-γ2	22.5	(0.1)	26.9	(0.2)						0	2.5	
Val333-γ1	13.1	(0.2)	15.5	(0.3)						0	1.8	
Leu337-δ2	7.8	(0.1)	5.7	(0.5)						0	3.7	
Val343-γ1	15.3	(0.1)	18.4	(0.1)						0	1.1	
Val343-γ2	9.4	(0.4)	9.4	(0.6)						0	3.5	
Val348-γ2	11.9	(0.1)	10.8	(0.2)						0	1.9	
Leu357-δ1	4.5	(0.1)	3.6	(0.2)						0	1.6	
Leu357-δ2	5.7	(0.1)	6.5	(0.3)						0	2.6	
Val361-γ1	5.6	(0.1)	5.2	(0.1)						0	3.6	
Val361-γ2	2.6	(0.1)	0.7	(0.2)						0	2.2	
Leu367-δ1	6.5	(0)	7.2	(0.1)						0	2.0	
Leu367-δ2	7.4	(0.1)	6.3	(0.1)						0	3.5	

$\chi^2(0)/\chi^2(ex)$ is the ratio of the χ^2 for a flat line over the χ^2 for fitted general 2-site exchange:
An F-critical value of 3.77 corresponds to a 99.99% confidence level.
$\chi^2(\Delta\omega H0)/\chi^2(\Delta\omega H)$ is the ratio of the χ^2 for a fit with fixed $\Delta\omega H=0$ over the χ^2 for a fit with varying $\Delta\omega H$:
An F-critical value of 2.03 corresponds to a 95% confidence level.
Model 1(2): fast (general) 2-site exchange.

Table S6. Global fit parameters 293K

Methyl	R_{20}(1/s) 500MHz		R_{20}(1/s) 800MHz		R_{ex}(1/s) 800MHz	k_{ex}(1/s)		$\Phi^{1/2}$ (s^{-1})	$\frac{\chi^2(g)}{\chi^2(i)}$
Leu77-δ1	35.2	(1.9)	52.7	(2.3)	8.7	2300	(120)	14.4 (3.6)	1.0
Ile87-δ1	28.3	(2.5)	30.8	(3.4)	3.3	"	"	8.9 (2.8)	1.0
Met109-ε	12.3	(4.7)	12.1	(5.0)	16.4	"	"	19.7 (2)	1.0
Met112-ε	28.3	(2.5)	31.9	(3.4)	2.5	"	"	7.7 (3.9)	1.6
Leu119-δ2	18.2	(3.8)	18.8	(5.4)	3.2	"	"	8.8 (2.1)	1.2
Met120-ε	24.1	(2.9)	24.6	(4.2)	2.7	"	"	8 (2.7)	1.7
Met137-ε	32.1	(2.2)	34.1	(3.1)	3.5	"	"	9.1 (3.5)	1.3
Ile149-δ	24.7	(2.5)	35.5	(3.0)	20.2	"	"	21.9 (2.2)	1.0
Leu167-δ2	18.2	(3.8)	18.9	(5.4)	3.1	"	"	8.6 (2.1)	1.2
Met182-ε	10.8	(5.3)	13.3	(6.6)	14.8	"	"	18.8 (1.4)	1.1
Val186-γ2*	9.9	(6.8)	11.3	(8.9)	3.9	"	"	9.7 (1.3)	1.0
Val187-γ*	9.9	(6.8)	11.3	(8.9)	3.9	"	"	9.7 (1.3)	1.0
Ile209-δ	22.7	(2.8)	27.3	(3.6)	13.3	"	"	17.8 (2.1)	1.0
Met219-ε	31.4	(2.2)	31.2	(3.2)	5.0	"	"	11 (3.2)	1.5
Leu225-δ1	19.8	(2.1)	25.1	(2.5)	81.3	"	"	44 (2.5)	1.4
Met262-ε	18.9	(3.3)	25.4	(4.0)	15.9	"	"	19.5 (1.9)	1.9
Leu265-δ1	37.9	(1.8)	44.2	(2.5)	5.1	"	"	11 (4.1)	1.0
Leu288-δ1	27.8	(2.4)	36.2	(3.0)	11.0	"	"	16.2 (2.3)	1.0
Leu288-δ2	18.7	(3.7)	24.7	(4.7)	3.7	"	"	9.4 (2.5)	1.0
Met291-ε	25.6	(2.7)	25.3	(3.9)	4.7	"	"	10.5 (2.3)	1.4
Leu292-δ1	35.7	(1.9)	40.8	(2.5)	10.5	"	"	15.8 (2.6)	1.0
Leu294-δ2	31.6	(2.0)	56.0	(2.2)	23.4	"	"	23.6 (3.1)	1.1
Val300-γ1	8.9	(7.3)	8.8	(8.0)	4.9	"	"	10.8 (1.6)	1.1
Leu314-δ2	15.7	(4.4)	15.7	(4.9)	3.6	"	"	9.3 (3.3)	1.1
Val323-γ1	14.8	(4.7)	19.2	(6.1)	2.2	"	"	7.2 (2.5)	1.0

k_{ex} was fit globally with a 2-site fast exchange model. $\chi^2(g)/\chi^2(i)$ is the ratio of the χ^2 of a global fit to the χ^2 of an individual fit. A global fit with a ratio > 2.0 is considered to be a worse model than an individual fit.
* V186γ2 & V187γ peaks overlap

Table S7. Global fits for BIRB796 at 293K

Methyl	R_{20}(1/s) 500MHz		R_{20}(1/s) 800MHz		R_{ex}(1/s) 800MHz	k_{ex}(1/s)		$\Delta\omega_c$ (s^{-1}) [$\Phi^{1/2}$ (s^{-1})]	p_B(%)	cluster	$\chi^2(1)/\chi^2(ini)$	$\chi^2(2)/\chi^2(ini)$
Val86-γ2	*14.0*	*(4.2)*	*15.2*	*(5.9)*	*5.6*	1900	(70)	[7.6 (1.1)]		1	*1.0*	
Met137-ε	*36.1*	*(1.7)*	*39.6*	*(2.5)*	*3.7*	"	"	[6.2 (2.7)]		1	*1.1*	
Ile149-δ	*20.3*	*(3.0)*	*25.3*	*(4.0)*	*4.4*	"	"	[6.7 (2.9)]		1	*1.0*	
Val186-γ2	*13.9*	*(4.2)*	*18.8*	*(5.3)*	*7.2*	"	"	[8.6 (1.2)]		1	*1.0*	
Val187-γ	*13.3*	*(4.3)*	*18.5*	*(5.4)*	*8.0*	"	"	[9.1 (0.8)]		1	*1.0*	
Ile209-δ	*23.4*	*(2.6)*	*27.2*	*(3.5)*	*6.4*	"	"	[8.1 (1.5)]		1	*1.1*	
Leu225-δ1	*25.0*	*(1.6)*	*35.0*	*(1.9)*	*99.5*	"	"	[35.5 (1.8)]		1	*1.8*	
Met262-ε	*22.5*	*(2.6)*	*29.3*	*(3.3)*	*12.2*	"	"	[11.3 (1.7)]		1	*1.0*	
Leu288-δ1	*30.8*	*(1.9)*	*41.2*	*(2.4)*	*13.5*	"	"	[11.8 (1.8)]		1	*1.0*	
Met291-ε	*27.5*	*(2.2)*	*28.7*	*(3.3)*	*4.2*	"	"	[6.5 (1.9)]		1	*1.4*	
Leu292-δ1	*40.4*	*(1.4)*	*52.6*	*(1.8)*	*25.5*	"	"	[16.5 (1.8)]		1	*1.8*	
Val300-γ1	*10.7*	*(5.3)*	*13.6*	*(6.9)*	*6.7*	"	"	[8.3 (1.0)]		1	*1.1*	
Leu314-δ2	*16.6*	*(3.7)*	*20.8*	*(4.9)*	*4.1*	"	"	[6.4 (1.6)]		1	*1.1*	
Leu119-δ2	*22.6*	*(7.3)*	*25.4*	*(11.2)*	*3.8*	310	(60)	52.6 (10.3)	0.90	*2*	***2.1***	*1.1*
Met120-ε	*25.8*	*(10.2)*	*28.4*	*(16.6)*	*3.3*	"	"	44.9 (6.6)	"	*2*	***2.5***	*1.0*
Met219-ε	*34.5*	*(6.6)*	*37.5*	*(10.0)*	*4.5*	"	"	72.3 (12.9)	"	*2*	***3.0***	*1.1*

Exchange parameters were fit globally to a 2-site exchange model. $\chi^2(\#)/\chi^2(ini)$ is the χ^2 of a global fit (1 or 2) over the χ^2 of an individual fit. A ratio > 2.0 is considered to be a worse model than an individual fit.

Table S8. High-resolution PDBs with 30% or greater sequence identity to p38γ

PDBID and CHAIN					
1E9H A	3MI9 A	5DN3 A	1OVE A	3FMH A	4AAC A
1H1P A	3MY5 A	5DNR A	1OZ1 A	3FMJ A	4DLI A
1H1Q A	3PY3 A	5DT3 A	1R39 A	3FMK A	4DLJ A
1H1R A	3QHR A	5EFQ A	1R3C A	3FML A	4E5A X
1H1S A	3QHW A	5G1X A	1W7H A	3FMM A	4E5B A
1H24 A	3TNW A	5HLP A	1W84 A	3FMN A	4E6A A
1H25 A	4BCK A	5LI1 A	1WFC A	3FSF A	4E6C A
1H26 A	4BCM A	5LI9 A	1YWR A	3FSK A	4EH2 A
1H27 A	4BCN A	5LMK A	1ZYJ A	3GC7 A	4EH5 A
1JST A	4BCO A	5LXM A	1ZZ2 A	3GFE A	4F9Y A
1JSU A	4BCP A	5ORL A	1ZZL A	3HA8 A	4KIN A
1OGU A	4BCQ A	5ORN A	2FSL X	3HL7 A	4KIP A
1OI9 A	4BN1 A	5ORO A	2FSO X	3HLL A	4KIQ A
1OIU A	4CEG A	5ORP A	2FST X	3HP2 A	4LOO A
1OIY A	4CFN A	5ORR A	2GFS A	3HP5 A	4LOP A
1OL5 A	4CFU A	5ORS A	2GHL A	3HRB A	4LOQ A
1P5E A	4CFV A	5ORT A	2GHM A	3HUB A	5MTX A
1PKD A	4CFW A	5ORV A	2I0H A	3HVC A	5MTY A
1QMZ A	4DC2 A	5ORW A	2OKR A	3ITZ A	5N63 A
1W98 A	4EOI A	5ORX A	2QD9 A	3KF7 A	5N65 A
2A19 A	4EOJ A	5ORY A	2RG5 A	3L8X A	5N67 A
2CCH A	4EOK A	5ORZ A	2RG6 A	3LFA A	5N68 A
2CJM A	4EOL A	5OS0 A	2Y8O A	3MGY A	5O8U A
2ERK A	4EOM A	5OS1 A	2YIX A	3MH0 A	5O8V A
2G9X A	4EON A	5OS3 A	2ZAZ A	3MH2 A	5O90 A
2I0E A	4EOO A	5OS4 A	2ZB0 A	3MPA A	5TBE A
2IW6 A	4EOP A	5OS5 A	2ZB1 A	3MPT A	5TCO A
2IW8 A	4EOQ A	5OS6 A	3BX5 A	3MVM A	5UOJ A
2IW9 A	4EOR A	5OSD A	3COI A	3NEW A	5XYY A
2UZE A	4EOS A	5OSE A	3FC1 X	3NWW A	
2UZL A	4EWQ A	5OSF A	3FI4 A	3P4K A	
2WMB A	4I3Z A	5V60 A	3FKL A	3RIN A	
3A8W A	4II5 A	5V61 A	3FKN A	3ROC A	
3A8X A	4IZA A	5V62 A	3FKO A	3S3I A	
3BHT A	4MYG A	1DI9 A	3FL4 A	3S4Q A	
3BHU A	4NM5 A	1IAN A	3FLN C	3U8W A	
3BHV A	4NST A	1LEW A	3FLQ A	3UVP A	
3BLH A	4WNO A	1LEZ A	3FLS A	3UVQ A	
3DDQ A	4WNP A	1M7Q A	3FLW A	3ZSH A	
3E5A A	5CI7 A	1OUK A	3FLY A	3ZYA A	
3HA6 A	5CYI A	1OUY A	3FLZ A	4AA4 A	

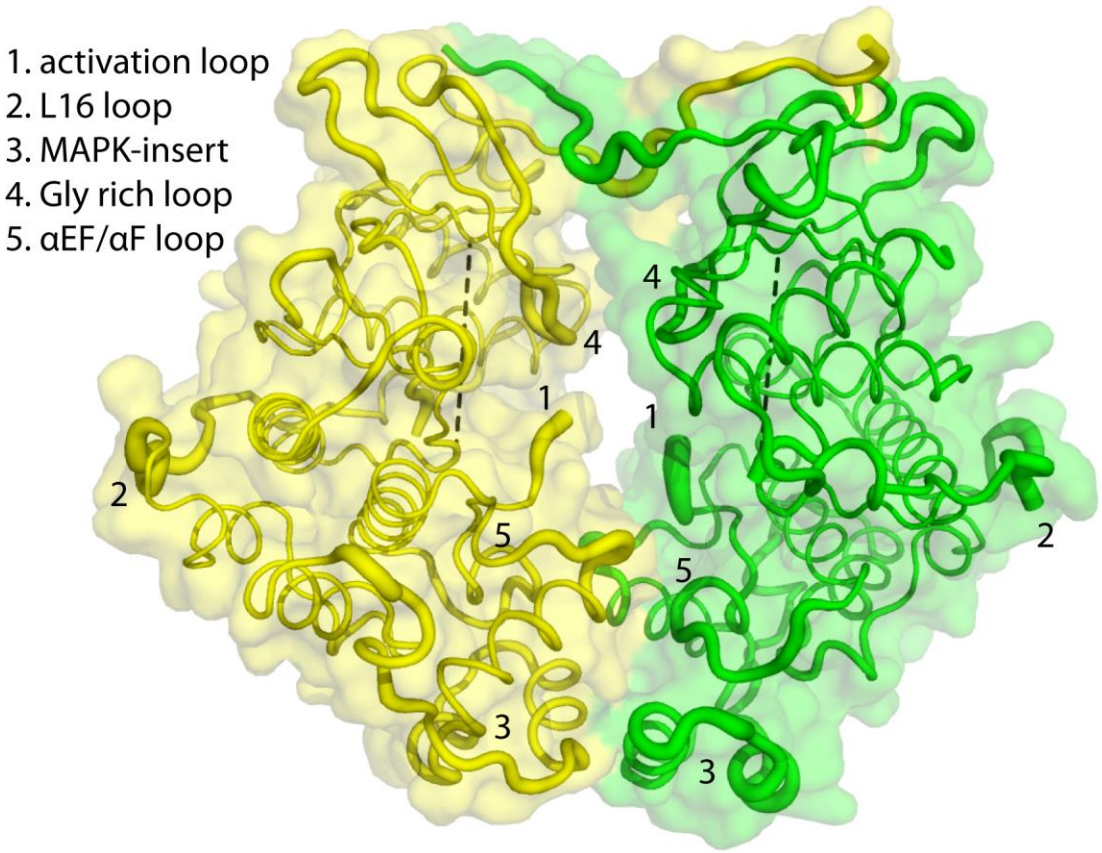

Figure S1. Crystal structure of human inactive apo p38γ at 2.55Å resolution. The two molecules in the asymmetric unit are shown in green (open) and yellow (compact). The extent of compaction is measured by the distance between K56 and Asp153, as indicated by the dashed lines (10.1 Å for compact and 12.5 Å for open). Electron density is absent for the activation loop, residues 177 to 187, in both molecules. Similarly, no density is found for residues 315 to 321, leading up to the L16 loop in molecule 1, while weak density is observed for these residues in molecule 2. Relatively high B-values, as represented by the thickness of the backbone trace, are observed in the MAPK-insert, αEF/αF loop, and glycine rich loop, suggesting that these regions are more flexible.

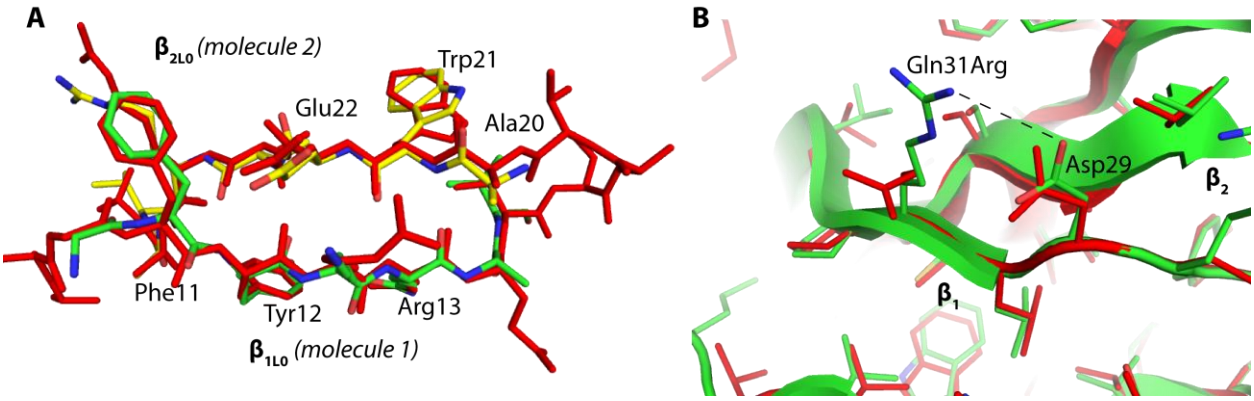

Figure S2. A. The β-strand swap does not perturb the structure of p38γ. The structure of activated p38γ, 1CM8, (red) aligned to β1L0, the swapped strand, of the open molecule (green) in the crystal structure of apo p38γ has very similar interactions and orientation relative to the non-swapped β2L0 from the compact molecule (yellow). In fact, the swapped strands are in the same orientation and make the same interactions as if they were not swapped. Excluding the β strand swap, the buried surface area between molecules in the asymmetric unit is only 622Å^2 out of 17,300Å^2 of total surface area, suggesting that strand swap may not have biological significance. B. The spontaneous Gln31Arg mutation in the β1 strand is within hydrogen-bond distance of the side chain of Asp29, stabilizing the local structure. For comparison, the crystal structure of activated p38γ is shown in red. In the crystal structure of the activated protein, the β1 strand and loop are partially disordered.

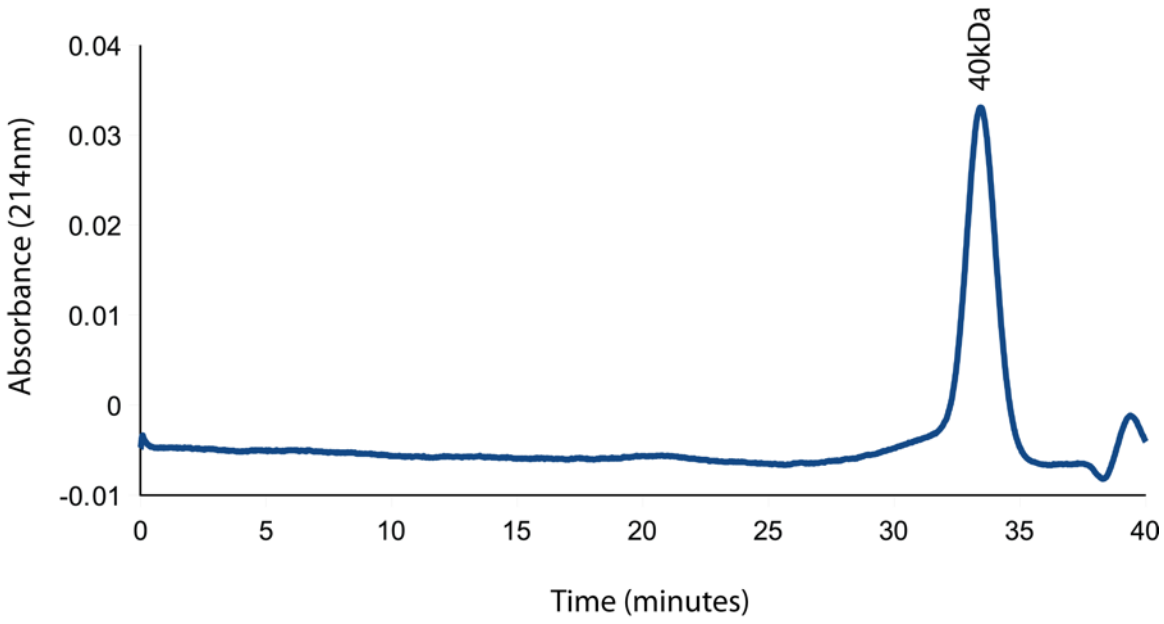

Figure S3. S75 analytical size exclusion chromatography of inactive p38γ(7-352) shows that it exists mainly as a monomer in solution with MW ~ 40kDa based on comparison to standard proteins.

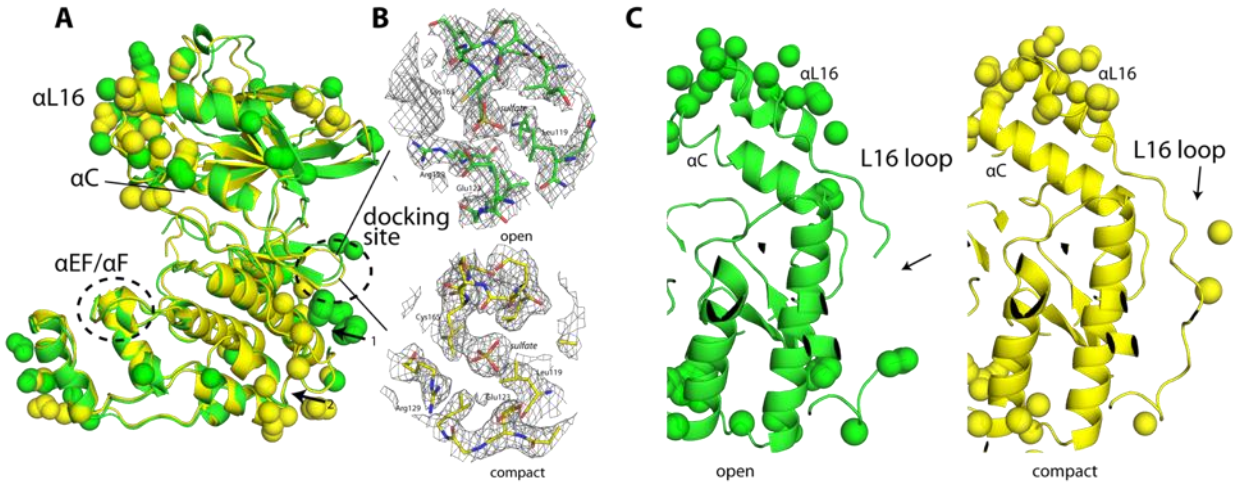

Figure S4. A. Crystal lattice contacts (shown as spheres) are similar for the molecules displaying open and compact conformations. Open (green) and compact (yellow) conformations are overlaid. Typically, the αEF/αF loop becomes reorganized upon activation.[1] Here, no reorganization is seen between the open and compact models. Any differences in the crystal contacts in the neighboring MAPK-insert thus do not cause changes in the αEF/αF conformation. The compaction seen between the apo and active-like structures is not driven by αEF/αF reorganization. B. Electron density (2Fo-Fc) in the docking-site for open and compact structures. A sulfate group is modeled into the density. Near identical contacts are made in both conformations. C. Crystal lattice contacts (shown as spheres) at the N-terminal portion of the L16 loop are observed in the compact structure (yellow) but not in the open structure (green) where this region has poor electron density and a model cannot be built.

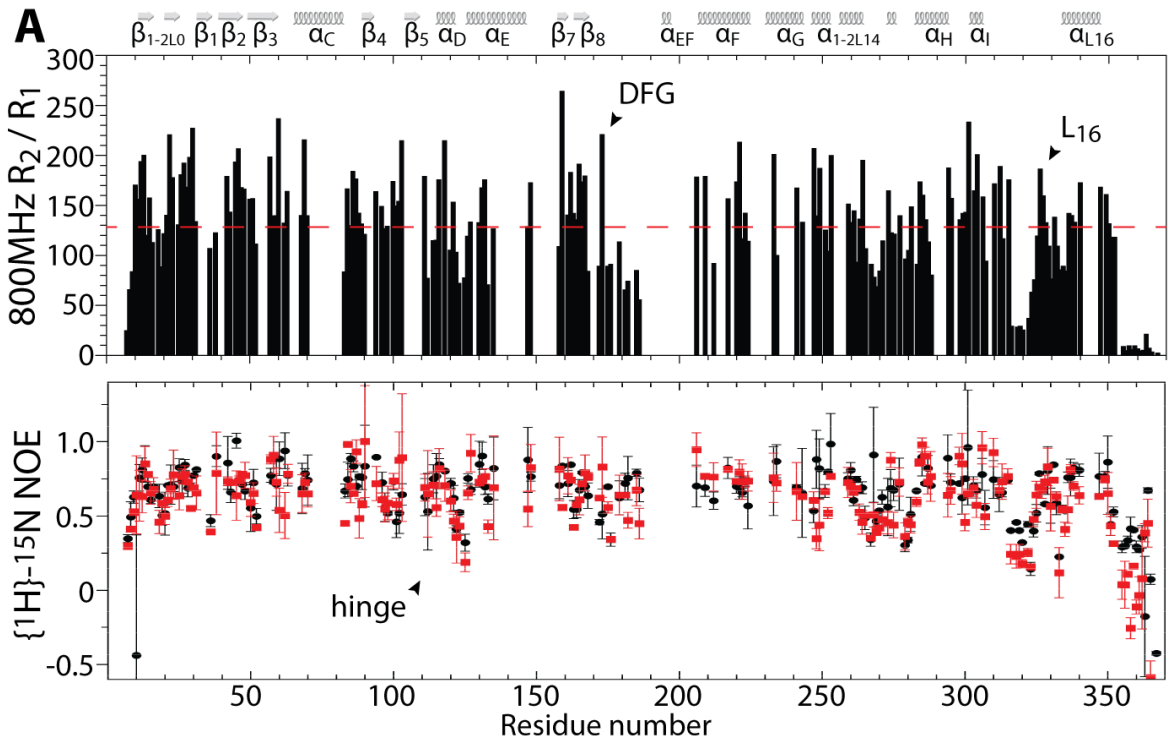

Figure S5. ^{15}N relaxation data collected at two magnetic fields. The R_2/R_1 ratio at 800MHz (upper panel) and the {^{1}H}-^{15}N heteronuclear NOE (lower panel) at 500MHz (red) and 800MHz (black) are shown as a function of residue number. Higher heteronuclear NOEs indicate that backbone motions on the ps-ns time scale are restricted while lower values are indicative of flexibility. Flexible regions are observed between secondary structure elements (indicated at the top of the figure), in particular in the hinge between lobes. Regions with elevated (depressed) R_2/R_1 typically undergo slower (faster) processes; this is observed for residues in the DFG loop (Gly173) and L16 loop (residues 326-328). The red dashed line marks the mean R_2/R_1.

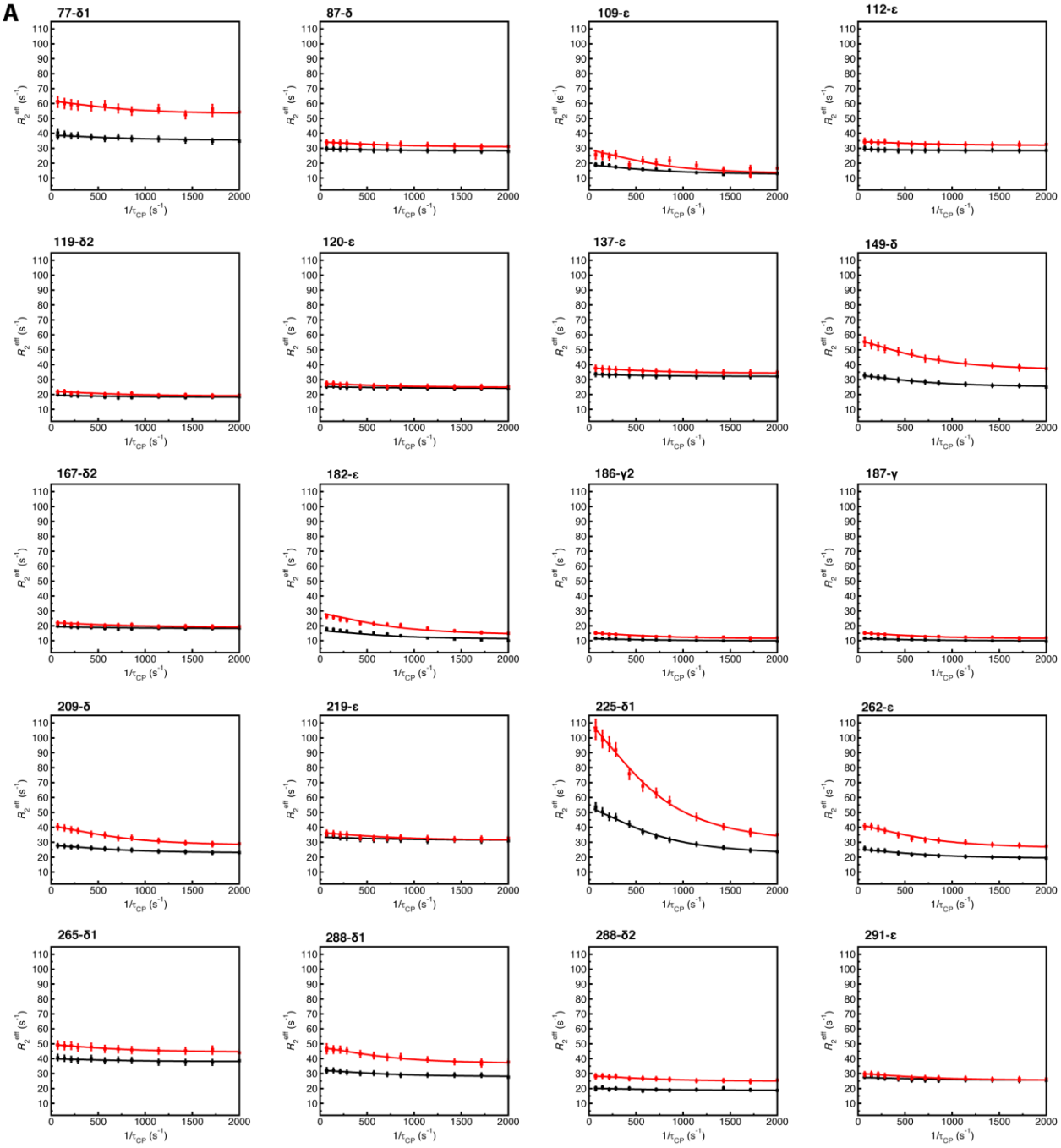
A
77-δ1
87-δ
109-ε
112-ε
119-δ2
120-ε
137-ε
149-δ
167-δ2
182-ε
186-γ2
187-γ
209-δ
219-ε
225-δ1
262-ε
265-δ1
288-δ1
288-δ2
291-ε
R_2^{eff} (s^{-1})
$1/\tau_{CP}$ (s^{-1})

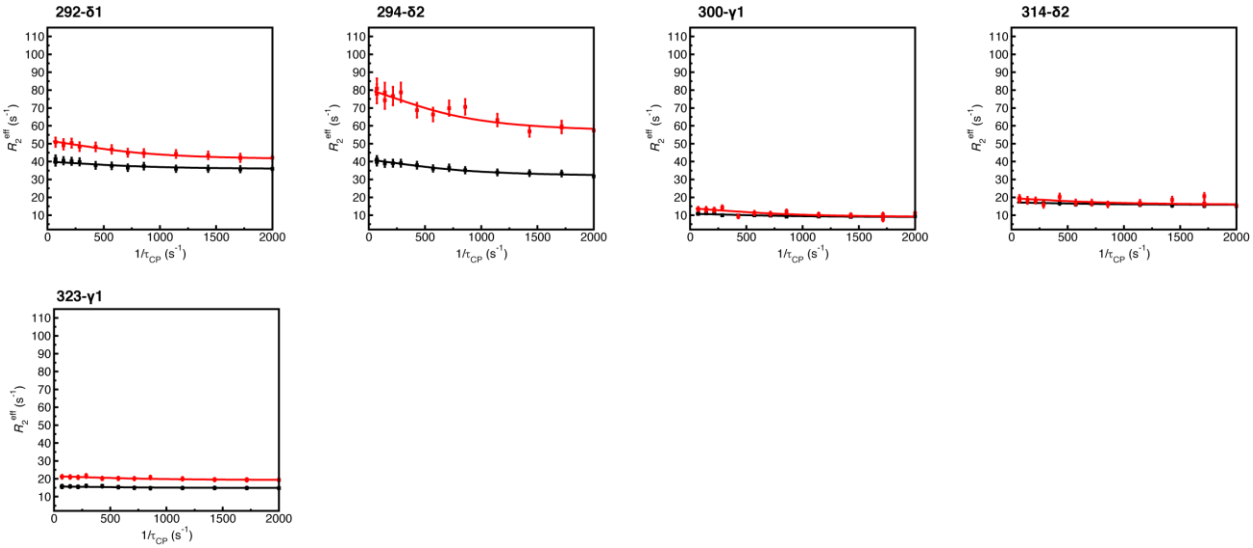
292-δ1
294-δ2
300-γ1
314-δ2
323-γ1
R_2^{eff} (s^{-1})
$1/\tau_{CP}$ (s^{-1})

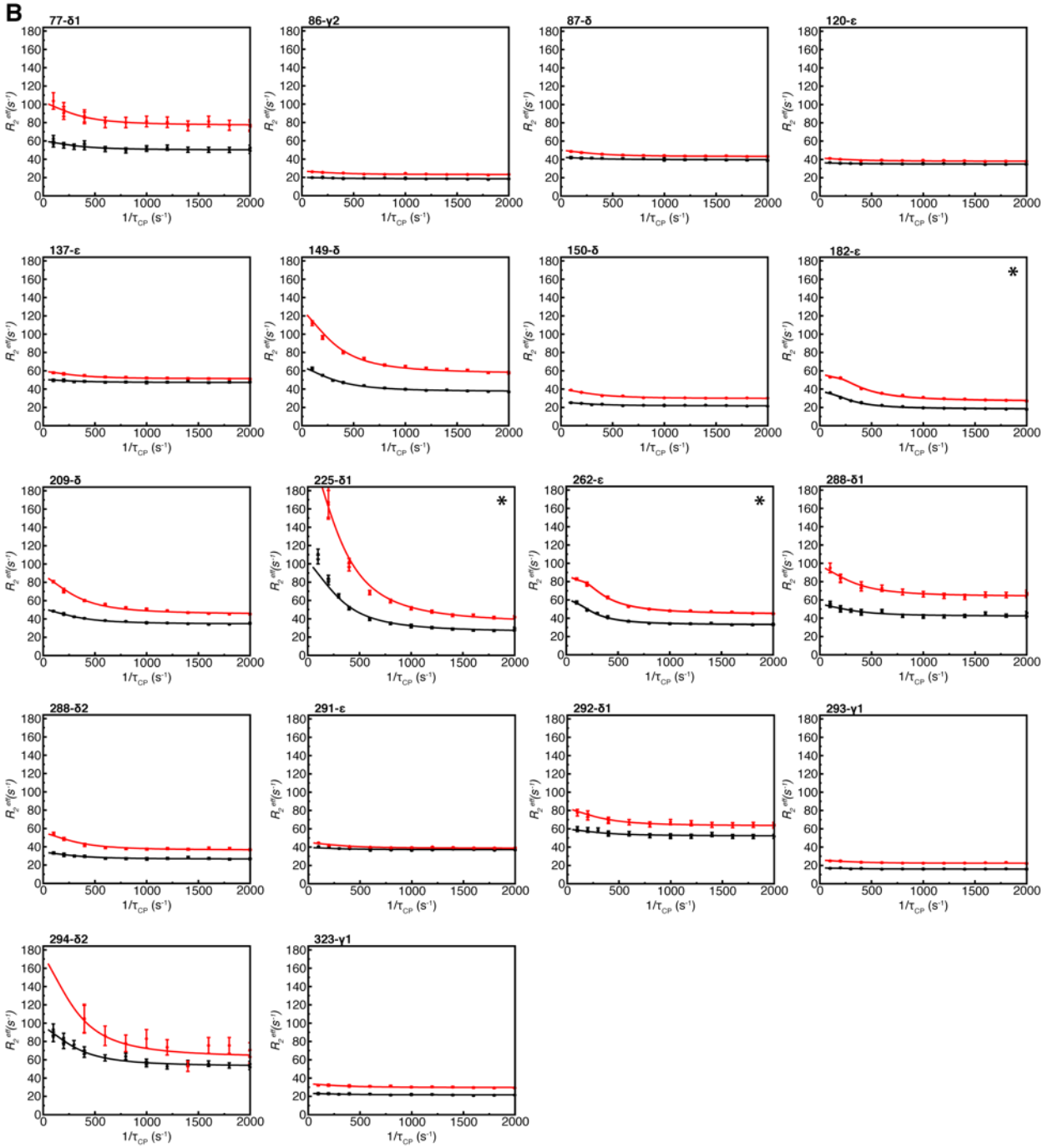
B
77-δ1
86-γ2
87-δ
120-ε
137-ε
149-δ
150-δ
182-ε
209-δ
225-δ1
262-ε
288-δ1
288-δ2
291-ε
292-δ1
293-γ1
294-δ2
323-γ1
$R_2^{eff}(s^{-1})$
$1/\tau_{CP}$ (s^{-1})

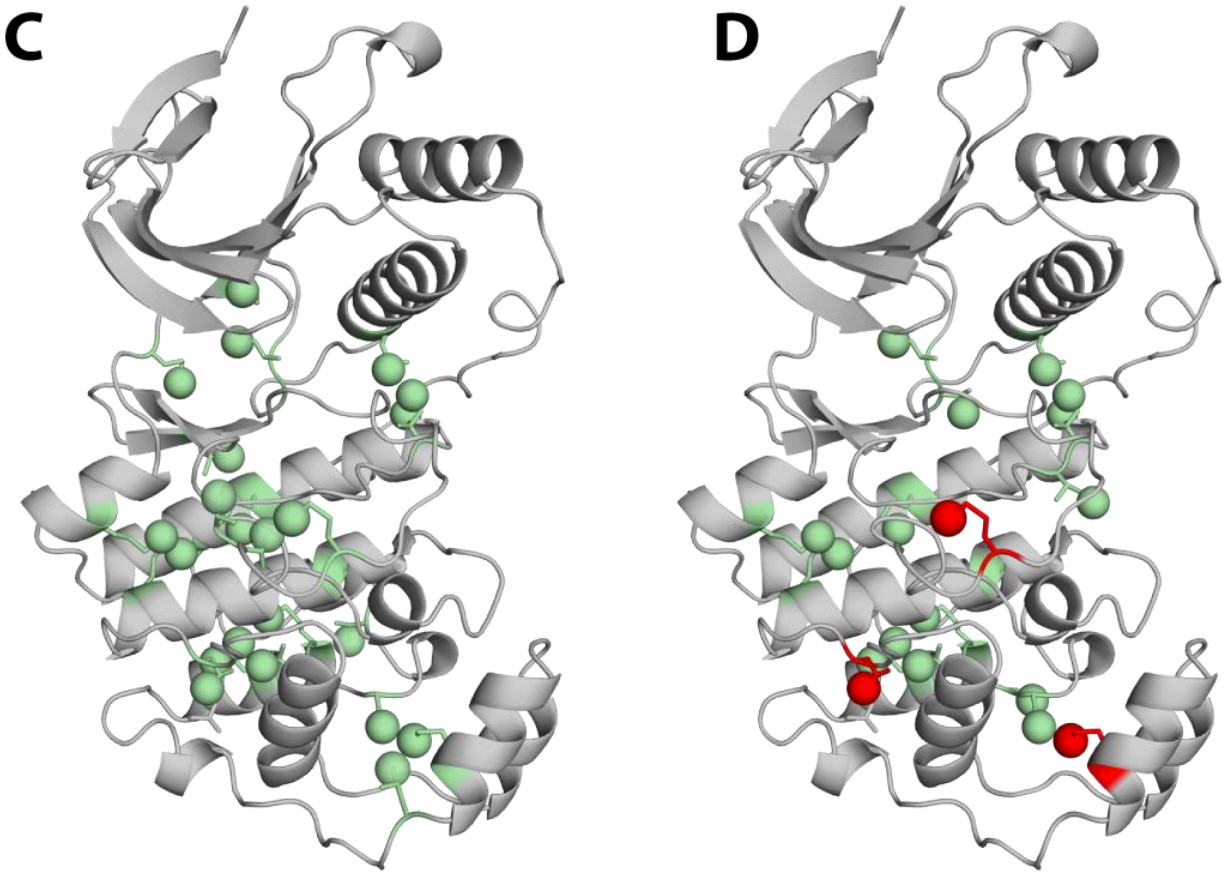

Figure S6. Globally fit methyl ^{13}C-^{1}H multiple quantum relaxation dispersion profiles at 800 MHz (red) and 500 MHz (black) at temperatures of (A) 293K and (B) 283K. Weak dispersive behavior at 293K is amplified by reducing temperature, suggesting the exchange process is on the faster end of the CPMG time scale (ms to μs). The dispersion curves for most residues were fitted to a global 2-site exchange process with a k_{ex} of 2300 s^{-1} (+/-120) at 293K and 960 s^{-1} (+/-30) at 283K. Dispersion curves that do not fit the global exchange process at 283K (marked with an asterisk) have fitted exchange rates < 690 s^{-1}. (C) Methyl groups that fit the global exchange process at 293K are shown as green spheres on the p38γ structure. (D) Methyl groups that report on the 960 s^{-1} (+/-30) conformational exchange process at 283K are shown as green spheres; methyls shown as red spheres report on a slower exchange process (Table 1).

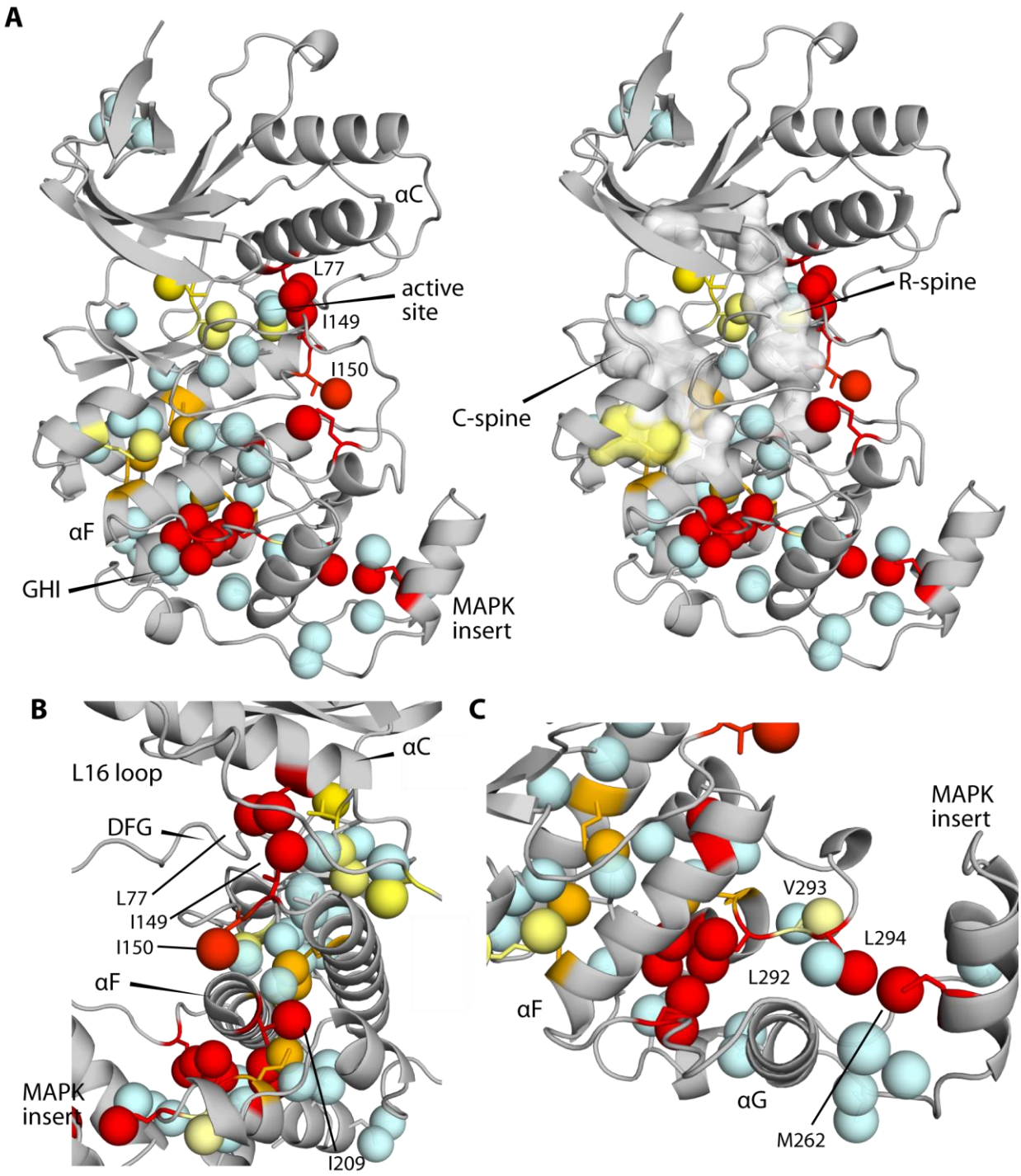

Figure S7. Methyl probes (shown as spheres) reveal a network of dynamics in the core of p38γ. (A) Exchange contributions (R_{ex}) at 293K and 800MHz are plotted on a linear scale from yellow to red. Cyan spheres represent methyls with a large difference in R_{20} between the two fields at

293K (>5 s^{-1}, Table S5) suggestive of conformational exchange occurring on a timescale outside the limits of detection in CPMG experiments. Methyls undergoing conformational exchange span p38γ and are mostly associated with allosteric networks, previously identified by network analysis of chemical shift perturbations,[2] which run along spatially conserved hydrophobic allosteric spines, shown as surfaces in the right hand panel. (B) Location of methyl groups that report on conformational exchange in regions spanning from the L16-loop and αC-helix (L77), through the active site, (around the R-spine I149, I150), to the F-helix (I209) and GHI subdomain (L288, M291, L292). (C) Methyls displaying conformational exchange form a continuous network from the GHI subdomain to the MAPK-insert (V293, L294, M262).

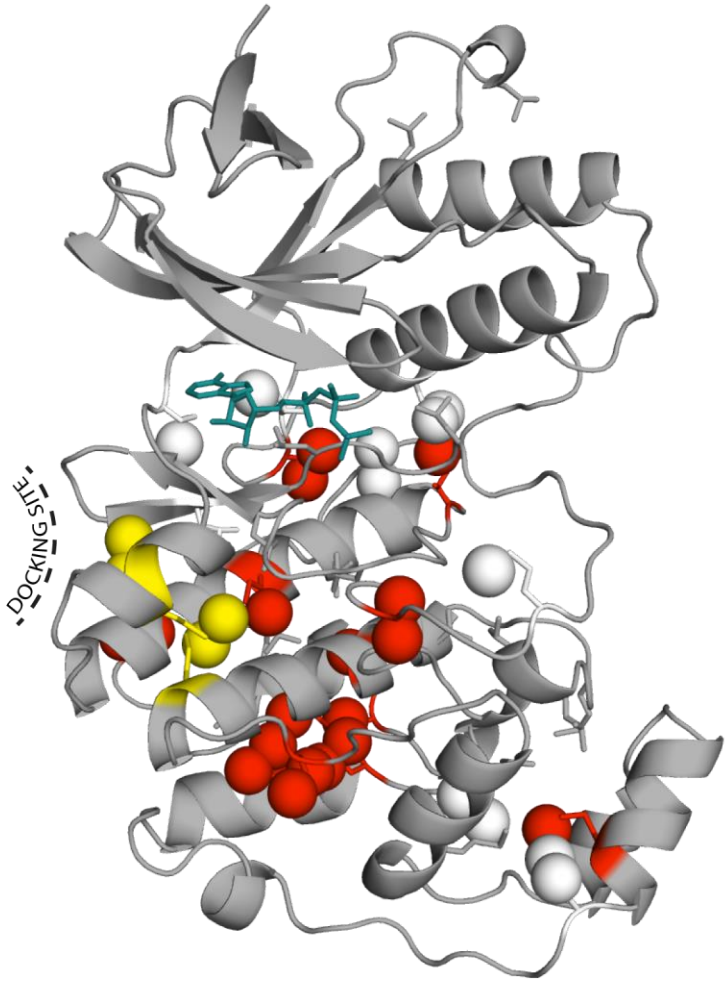

Figure S8. Cluster fit exchange rates for BIRB796 + p38γ. Red indicates the 2200 s^{-1} process, yellow the slower exchange at 280 s^{-1}. BIRB796 is modeled in the apo structure in teal. Inhibitor binding bridges a conserved set of hydrophobic residues from the N and C-lobes (including docking site residues). Coupling of the inhibitor binding to the docking site may contribute to the slow dynamics (yellow).

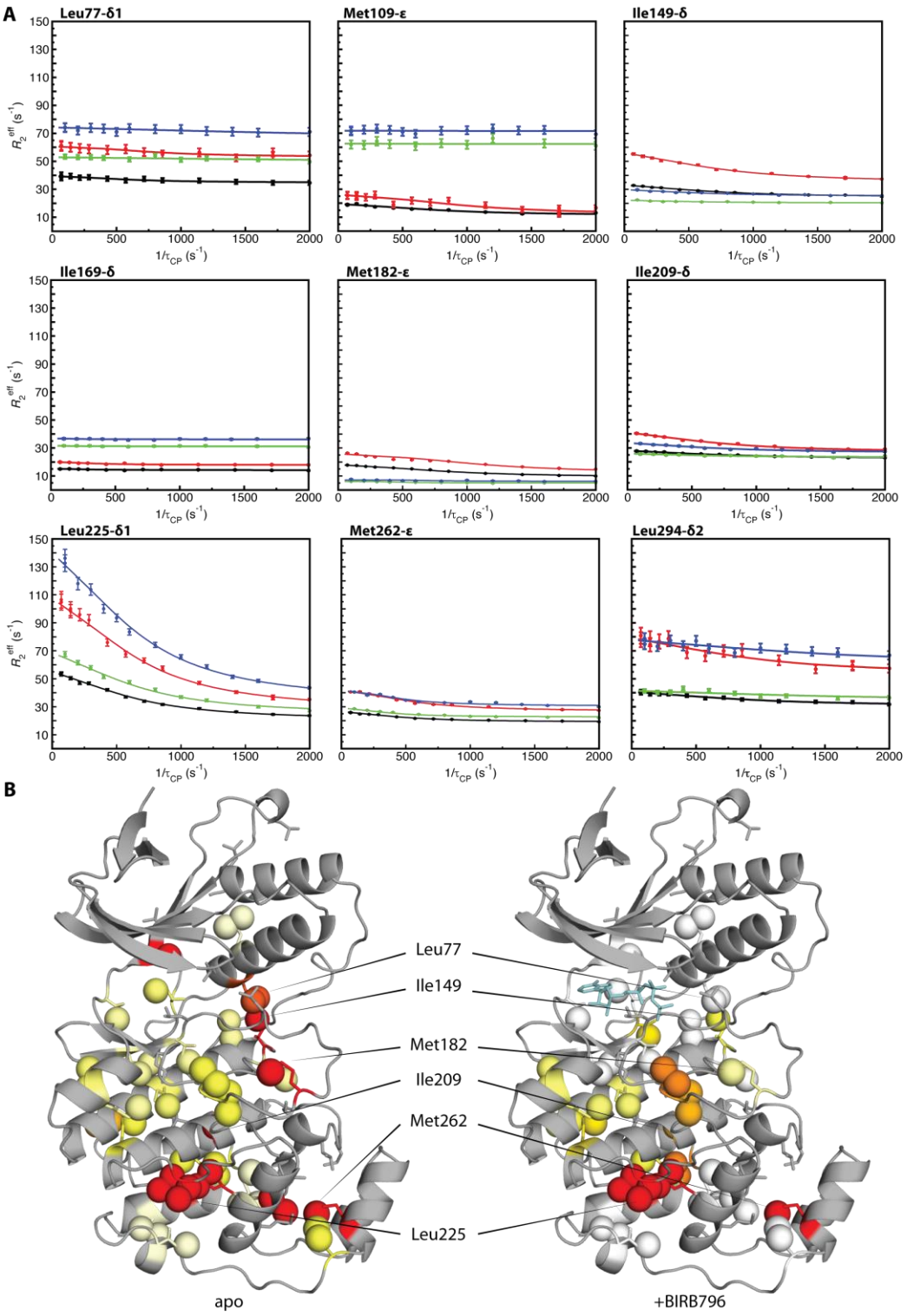

Figure S9. Effect of BIRB796 on methyl ^{13}C-^{1}H multiple quantum relaxation dispersion of apo p38γ. (A) Relaxation dispersion profiles for a subset of residues in apo p38γ (at 500MHz, black

and 800 MHz, red) are compared to those for the BIRB796 complex (at 500 MHz, green and 800 MHz, blue) at a temperature of 293K. Representative loss of dispersion is shown for Ile149, Met182, Ile209, and Leu294. This loss of conformational exchange can be attributed to loss of concerted DFG-hairpin formation and compaction. Methyls of Leu 77, Met109, and Ile169 near the BIRB796 binding site show a change in the timescale of dynamics exhibiting a loss of measurable R_{ex} but an increase in R_{20}. (B) The loss of dynamics follows the allosteric network described in Fig. S7. Small change in dispersion is seen for Met262 in the MAPK insert. This residue was not a part of the global process described for the apo-inactive state at 283K. Increases in the magnitude of R_{ex} are seen for some residues such as Leu225 (which was also not a part of the global process in the uninhibited state at 283K). R_{ex} is plotted on the structure of p38γ,. R_{ex} is shown for apo(left) and +BIRB796(right) on a continuous color scale from white (no R_{ex}) to yellow (R_{ex} = 4.0 s^{-1}) to red (R_{ex} > 6.0 s^{-1}). The structure of apo p38γ with all loops modeled is used; the inhibitor (cyan bonds) has been modeled into the apo structure.

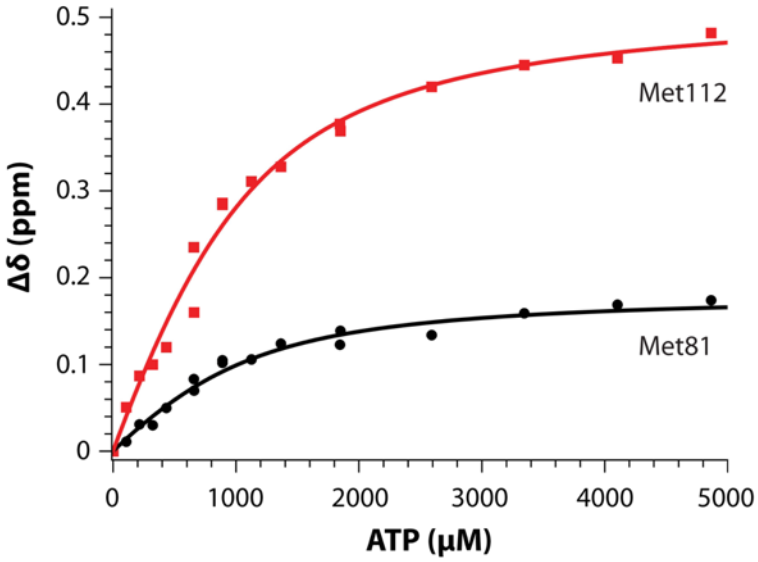

Figure S10. Changes in ^{1}H-^{13}C weighted average chemical shift upon binding of ATP to 200μM apo p38γ. Chemical shift differences were fitted to a binding curve using the program nmrKd.[3] The chemical shift difference was calculated as $\Delta\delta$ (ppm) = $[\Delta\delta H^2 + (\Delta\delta C/5.4)^2]^{1/2}$

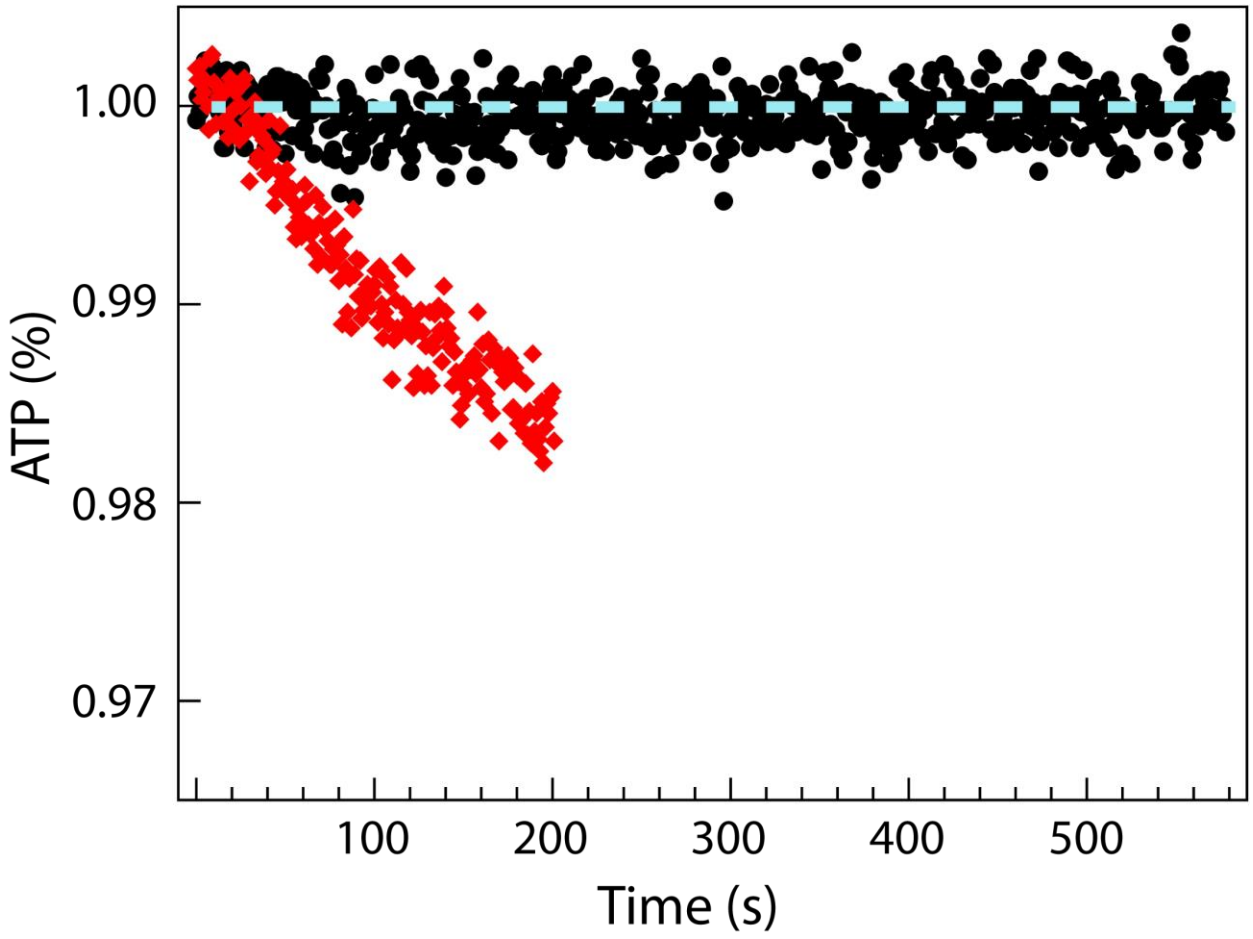

Figure S11. ATPase assay of p38γ. The ATPase activity of inactive p38γ was monitored by change in fluorescence of a coupled reporter system (NDP). The percent change in ATP concentration is shown versus time. Inactive p38γ had no measurable ATPase activity (black) at 295K, 50mM HEPES pH 7.6, 10mM $MgCl_2$, and 500uM ATP. The dashed cyan line illustrates the signal for 100% ATP. For comparison, the ATPase activity of activated p38γ is shown under the same conditions with a fit k_{cat}/K_M of ~7000 M^{-1} s^{-1} (red).

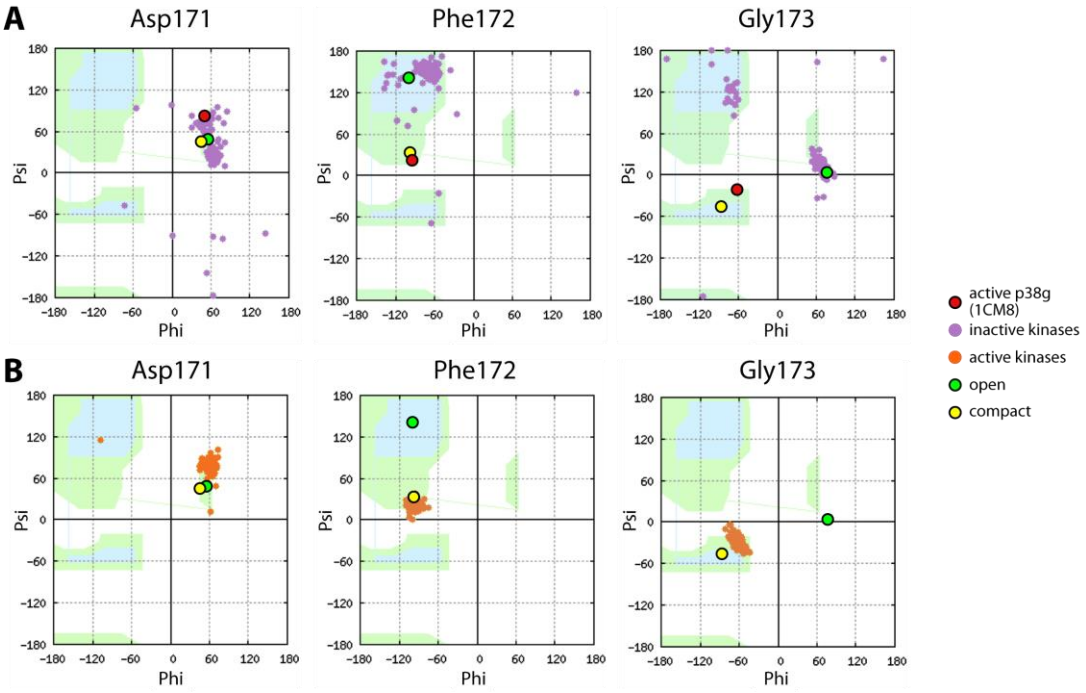

Figure S12. DFG pucker is a conserved feature of activated kinases. (A) The dihedral angles in the DFG loop of inactive p38 kinases (purple) are compared to those of activated p38γ (1CM8, red), the open conformation in the crystal structure (green), and the compact alternate conformation in the crystal structure (yellow). (B) The dihedral angles for the DFG loop of activated kinases with ≥30% sequence identity to p38γ (orange) are compared to those in the open conformation (green) and the compact conformation (yellow). The structures of the activated kinases have common Phe172 and Gly173 dihedral angles, which lead to the DFG pucker described in the main text. In inactive states, p38 kinases have a wider distribution of Phe172 and Gly173 dihedral angles compared to activated kinases, illustrating the flexible nature of the DFG loop when inactive. Other inactive kinases (not shown) have dihedral angles that are similar to activated kinases, suggesting that these kinases utilize other mechanisms (such as αC position, ligand accessibility, external regulatory elements, etc) to maintain an open conformation and inactivity. Puckering of the DFG loop appears to be a requirement for an active eukaryotic kinase.

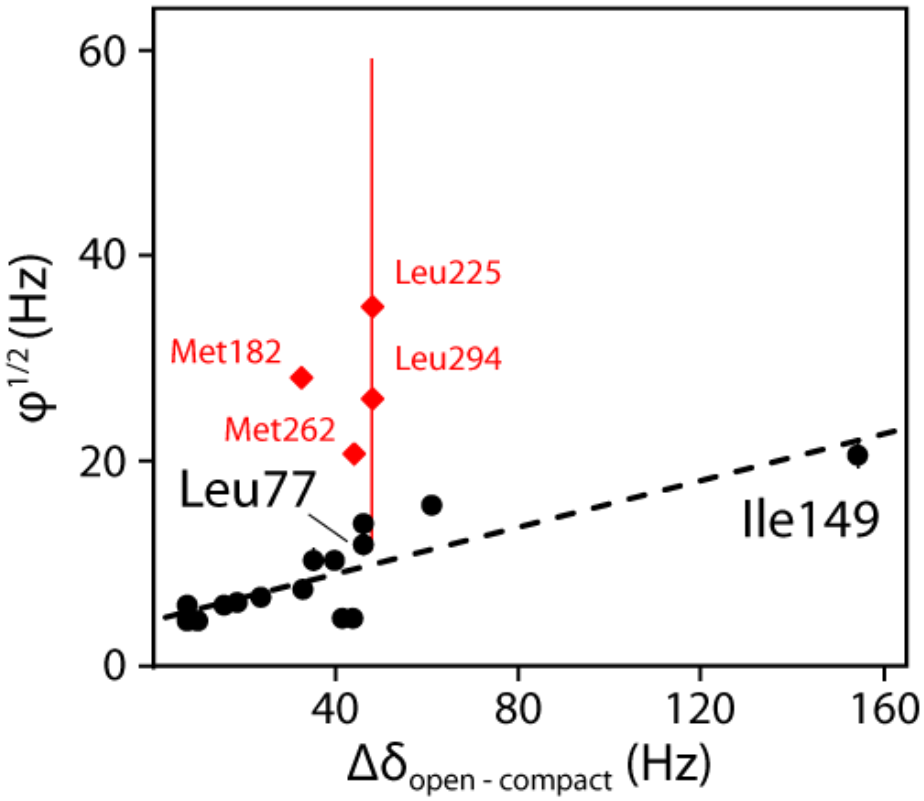

Figure S13. Correlation between chemical shift differences between the open and alternate conformer compact crystal structures predicted using SHIFTX2[4] and the parameter $\phi^{1/2} = (p_A p_B \Delta\omega_C^2)^{1/2}$ derived from the relaxation dispersion data at 283K (Table 1), where p_A and p_B are the populations of the two fitted states and $\Delta\omega_C$ is the carbon chemical shift difference. The linear correlation shown by the dashed line has $R^2 = 0.7$ (R=0.84). Residues in external loops whose dispersion data do not fit to the global exchange process (Leu225, Met262, and Met182 (red)) were excluded from the linear fit. Leu294 was also excluded since its methyl groups are in contact with Met262 in the MAPK insert and may experience exchange contributions from the slower process detected by Met262. Methyls reporting on a slower, non-global process are shown in red (Leu225, Met262, Met182). Leu294, which was excluded from the linear fit is also shown in red. Leu77 and Ile149, which probe the DFG loop and αC helix position are labeled.

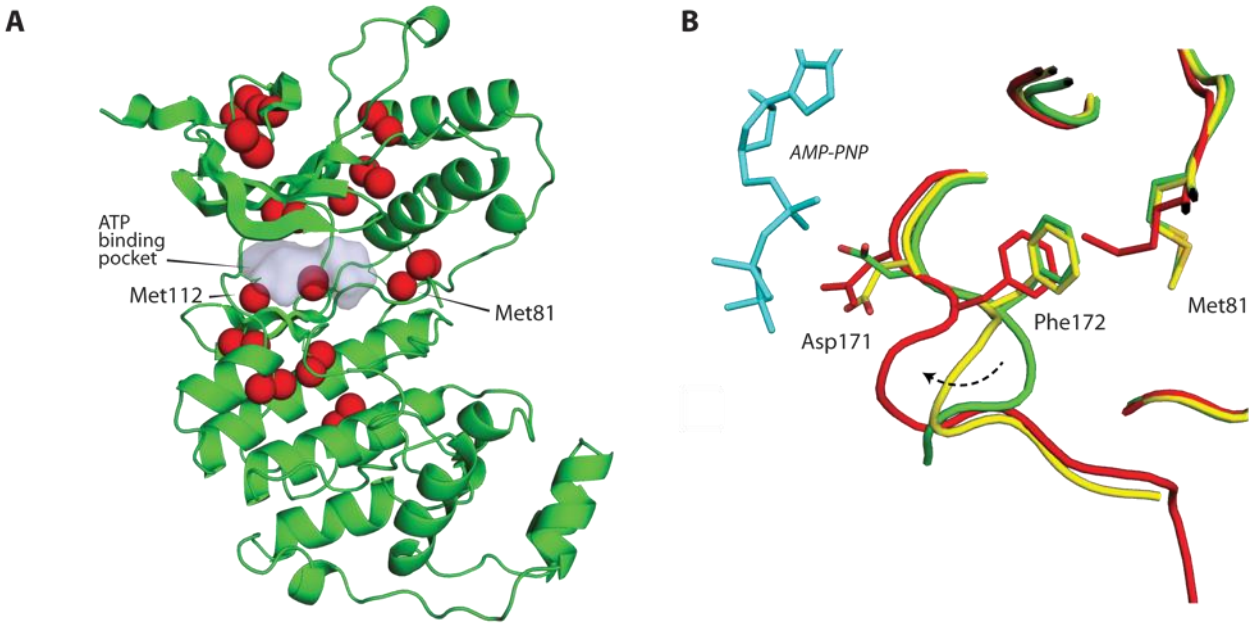

Figure S14. A. The structure of inactive p38γ showing residues with chemical shift perturbations due to ATP binding that are greater than 1 standard deviation above the mean (red). Shown are Met ε, Val γ1 and γ2, and Leu δ1 and δ2 methyls. B. ATP binding causes changes in the chemical shift of Met81, which does not contact ATP. ATP binding stabilizes Asp171 into a position that favors DFG loop pucker (open:green to compact/alternate conformer:yellow to activated:red, 1CM8[5]). This loop rearrangement leads to a change in the conformation of Phe172 which causes a large change in the chemical environment of Met81 (red, 1CM8).

References

(1) Tzarum, N., Eisenberg-Domovich, Y., Gills, J. J., Dennis, P. A., and Livnah, O. (2012) Lipid molecules induce p38α activation via a novel molecular switch, *J. Mol. Biol. 424*, 339-353.

(2) Aoto, P. C., Martin, B. T., and Wright, P. E. (2016) NMR characterization of information flow and allosteric communities in the MAP kinase p38γ, *Sci. Rep. 6*, 28655.

(3) Arai, M., Ferreon, J. C., and Wright, P. E. (2012) Quantitative analysis of multisite protein-ligand interactions by NMR: binding of intrinsically disordered p53 transactivation subdomains with the TAZ2 domain of CBP, *J. Am. Chem. Soc. 134*, 3792-3803.

(4) Han, B., Liu, Y., Ginzinger, S. W., and Wishart, D. S. (2011) SHIFTX2: significantly improved protein chemical shift prediction, *J. Biomol. NMR 50*, 43-57.

(5) Bellon, S., Fitzgibbon, M. J., Fox, T., Hsiao, H. M., and Wilson, K. P. (1999) The structure of phosphorylated p38γ is monomeric and reveals a conserved activation-loop conformation, *Structure 7*, 1057-1065.